D5.4 Final report on service elements for CO_2 emission and transport model integration

Anna Agustí-Panareda and

Dominik Brunner

Co-ordinated by ECMWF

D5.4 Final report on service elements for CO_2 Emission and Transport Model Integration

Dissemination Level: Public/

Author(s) : Anna Agustí-Panareda (ECMWF), Dominik Brunner (EMPA), Joe McNorton (ECMWF), Gianpaolo Balsamo (ECMWF), Jérôme Barré (ECMWF), Anton Beljaars (ECMWF), Souhail Boussetta (ECMWF), Frédéric Chevallier (LSCE), Margarita Choula (ECMWF), Hugo Denier van der Gon (TNO), Michail Diamantakis (ECMWF), Johannes Flemming (ECMWF), Sébastien Garrigues (ECMWF), Marc Guevara (BSC), Greet Janssens-Maenhout (JRC), Martin Jung (MPI-BGC), Thomas Kaminski (iLab), Andrzej Klonecki (SPASCIA) Maarten Krol (WU), Mark Parrington (ECMWF), Wouter Peters (WU), Pascal Prunet (SPASCIA), Sophia Walther (MPI-BGC)

Date: 02/102020

Version: 1.0

Contractual Delivery Date: 30/09/2020

Work Package/ Task: WP5/ T5.2

Document Owner: ECMWF

Contributors: ECMWF, EMPA, JRC, BSC, LSCE, iLab, MPI-BGC, SPASCIA, TNO, ULUND, WU

Status: Final

CHE: CO2 Human Emissions Project

Coordination and Support Action (CSA)
H2020-EO-3-2017 Preparation for a European capacity to monitor CO2 anthropogenic emissions

Project Coordinator: Dr Gianpaolo Balsamo (ECMWF)
Project Start Date: 01/10/2017
Project Duration: 39 months

Published by the CHE Consortium

Contact:
ECMWF, Shinfield Park, Reading, RG2 9AX,
gianpaolo.balsamo@ecmwf.int

The CHE project has received funding from the European Union's Horizon 2020 research and innovation programme under grant agreement No 776186.

Table of Contents

Figures

Tables

1 Executive Summary

The CHE prototype is designed to estimate carbon dioxide (CO_2) emissions using a modelling framework to link all the CO_2 relevant observations with prior knowledge of the anthropogenic emissions and other natural fluxes that affect the observed atmospheric CO_2 signal. The modelling aspects include atmospheric transport, atmospheric chemistry and land surface and ocean biogeochemical and transport processes, as well as statistical models of anthropogenic emissions of CO_2 and co-emitted species based on human activity data. A multi-scale, multi-species and multi-stream approach is required to target the various types of CO_2 emissions and natural fluxes, and their wide range of scales from point sources to cities, regions/ecosystems and countries. Different transport schemes suited for the different applications from local to global scales are listed and their challenges are described. The various approaches to estimate biogenic fluxes and anthropogenic emissions that serve as prior information are reviewed with their strengths and weaknesses. A comparison of the different transport models and prior datasets is proposed to assess the different capabilities of the models and priors used to perform the CHE library of simulations. Integration of the various components in the framework of Earth System Modelling is ongoing, with new developments on tracer transport modelling, simulations of plumes from emission hotspots, and urban modelling, among others. The full integration of the modelling and prior components towards a CO_2 Monitoring and Verification Support (MVS) capacity will be presented in a final report on the design of the CHE prototype.

2 Introduction

2.1 Background

The CHE prototype aims at building a system to monitor the exchange of carbon dioxide (CO_2) and potentially other important man-made greenhouse gases like methane (CH_4) between the Earth surface and the atmosphere with the use of observations (mostly in the atmosphere), models and prior information, as well as their uncertainties to leverage the different sources of information. The system is designed to support the Paris Agreement and follows the directive of the European Commission CO_2 Task Force (Pinty et al., 2017). The general strategy and rationale for the CHE prototype is provided in CHE D5.9, stemming from the discussions in the first WP5 workshop (Reading, 25-26 September 2019). The main challenges are addressed with the following recommendations:

- **Multi-scale** approach to monitor emission from point sources (power stations or industrial facilities), cities and countries using different model domains from global to regional and to local model resolutions (e.g. from 25km to 100m).
- **Multi-species** approach to detect and attribute the observed atmospheric signal to specific sources/sinks (e.g. natural and anthropogenic emissions with sectorial distribution).
- **Multi-stream** approach to support different applications and users with a near-real time (NRT) stream focusing on shorter synoptic timescales designed to provide early warnings and giving feedback to data producers, and a re-analysis stream that uses consolidated quality-controlled data, products and models with their associated uncertainties to estimate trends.

This report focuses on the modelling and prior components of the prototype. It complements the reports on Earth observations (CHE D5.2), data assimilation methodology (CHE D5.6) and uncertainty representation (CHE D5.8). Modelling and prior information encapsulate our current knowledge and understanding of physical (e.g. atmospheric transport), biological (e.g. photosynthesis and ecosystem respiration) and chemical processes (affecting co-emitted reactive species like nitrogen oxides (NO_x), carbon monoxide (CO) and methane (CH_4), as well as human activity (e.g. fossil fuel energy production) that control the CO_2 exchange between the earth surface and the atmosphere. This knowledge and information are crucial to fill the gaps in the observing system and connect observations with the CO_2 emissions and natural fluxes that need to be monitored.

The different model components and prior information of the emissions are shown in Figures 1 and 2. Some model components will play a role of observation operators (linking observations to CO_2 fluxes) and others will provide prior flux information in the data assimilation process described in CHE D5.6. The individual components can be either coupled or integrated together in the forward model configuration which propagates the information from the surface fluxes to the atmospheric CO_2 concentrations forward in time. In an offline system (Figure 1), the components are connected through input/output streams. The components are designed to be run separately without allowing for feedbacks. In online models (Figure 2) the components are fully integrated, ultimately becoming an Earth System Model. They share the mapping and input data, ensuring consistency between components and they can interact with each other, allowing for the representation of complex feedbacks. The degree of coupling or integration can vary between different models and configurations. Offline models are faster and not as costly to run as ESMs. Whereas online models based on prognostic equations can be used to predict the atmospheric CO_2 state forward in time from days (e.g. Agusti-Panareda et al., 2014) to decades (e.g. Friedlingstein et al., 2006).

Section 3 provides a detailed description of the essential components in the model and prior information for the prototype. The strategy for their implementation in the protype is outlined in section 3.1. The model components are grouped into atmospheric transport which affects all the atmospheric tracers (section 3.2) and prior fluxes and other processes (e.g. chemistry) which vary depending on the species (section 3.3). Model development is essential to ensure a more accurate interpretation of observations and a more accurate representation of prior information. For example, the hourly to daily variation of the CO_2 signal from biogenic fluxes and anthropogenic emissions is often correlated with the signal from atmospheric transport. These processes need to be understood and represented in the model to be able to interpret the high temporal and spatial variability in the observed CO_2. In this report, the different challenges are addressed by going through the different components in the model, listing their options for implementation in the prototype and the approaches to evaluate their accuracy. Recent developments on tracer transport modelling, plume simulations from emission hotspots, urban modelling and biogenic fluxes from vegetation are highlighted in section 4. Sections 5 and 6 list the immediate requirements for the implementation of the prototype by 2023 and the research needs for the next 5 to 10 years. A summary of the immediate priorities for further development in the prototype is provided in section 7.

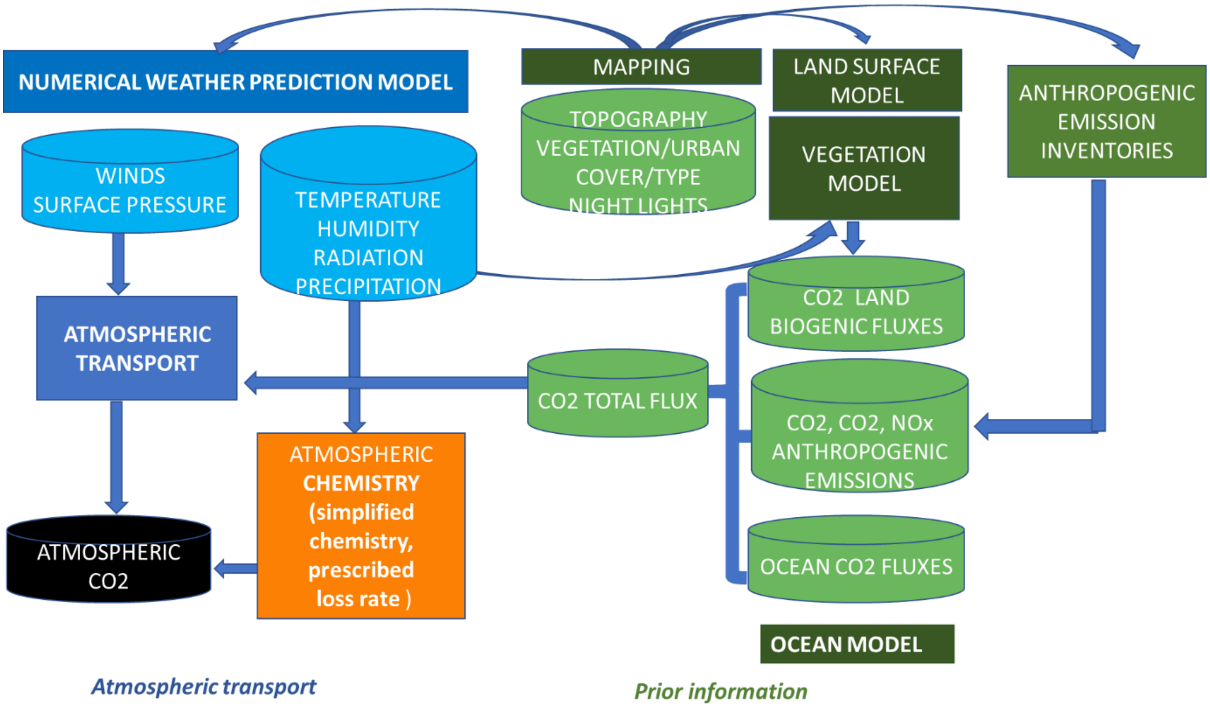

Figure 1 Offline approach to modelling and prior information provision with different components originating from independent models or products. The arrows denote the input/output channels of the different components (depicted as square boxes), which result in data products (in cylindrical shapes).

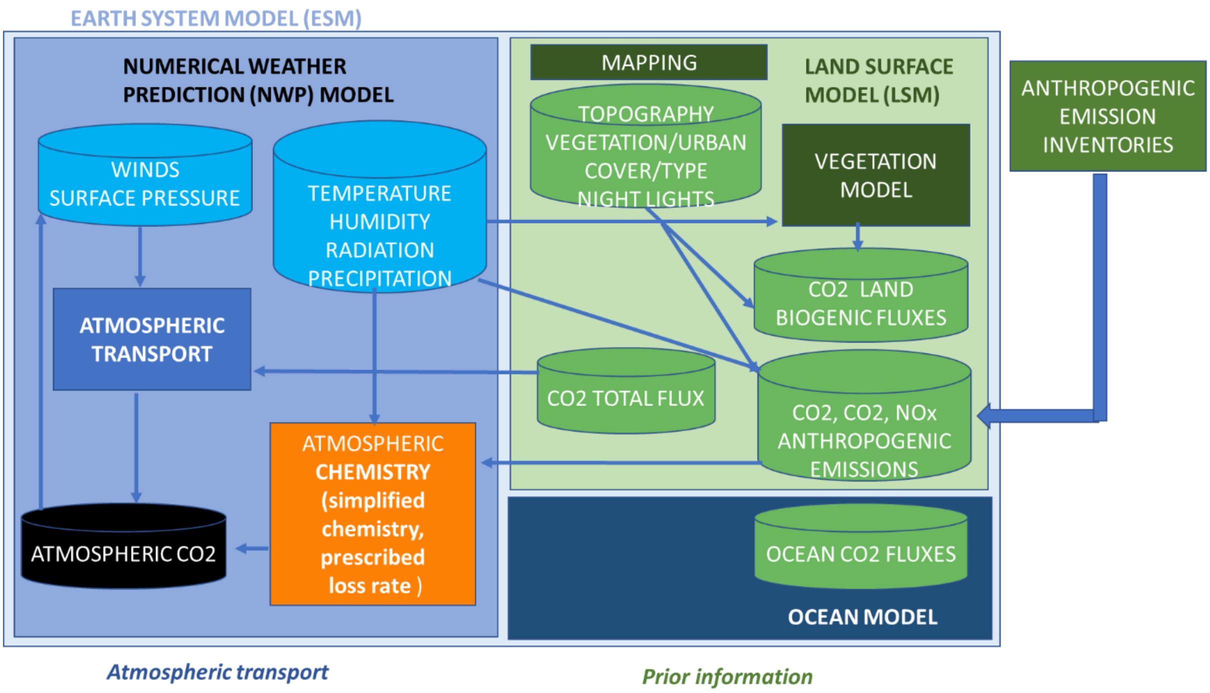

Figure 2 Online approach to modelling and prior information provision with different components integrated in Earth System Model. The same shapes are used as in Figure 1 to denote components and products. The input/output channels of the different components within the Earth System Model are depicted by thin arrows and the thicker arrow represents external inputs.

2.2 Scope of this deliverable

2.2.1 Objectives of this deliverables

In this report we will describe the strategy to represent the modelling and prior information aspects in the monitoring system. The different options for the modelling of transport and prior products for operational use and for research and development purposes are described. Finally, priorities for implementation by 2023 and for longer term research needs will be outlined, together with future plans for the final report, including the evaluation of the transport models and prior CO_2 fluxes used in the CHE nature runs.

2.2.2 Work performed in this deliverable

Synthesis of modelling aspects in CHE, CAMS, VERIFY and other ESA-funded projects as well as literature on carbon cycle and transport models.

2.2.3 Deviations and counter measures

Not applicable.

3 Modelling and prior components of the CHE prototype

3.1 Implementation strategy

The design of the CHE prototype requires the assessment of the different options for each component which depends on an implementation strategy. The implementation strategy for modelling and provision of prior information is based on three approaches:

- **HIGH RESOLUTION AND MULTI-SCALE CAPABILITY**

Given the wide range of scales of CO_2 signal (from point sources to hemispheric gradients), it is crucial to approach the problem with a high resolution and multi-scale monitoring capability (see D5.9). For prior anthropogenic emissions, point sources merit to be treated separately (e.g. power stations). Their total annual budget is usually well known and thus, it is distributed to the point source first, before applying a temporal scaling to modulate its variability on sub-annual timescales. The plumes from point sources will also require dedicated plume models, as global and regional models cannot resolve such small scales.

<u>EXAMPLES</u>: From global Numerical Weather Prediction (NWP) models to plume dispersion models focusing on hotspots

- **ONLINE AND COUPLED MODELLING CAPABILITY**

The observed atmospheric signal is a result of the interaction between the signal of the flux and the atmospheric transport. Because both fluxes and transport have a high spatial and temporal variability, they often co-vary. Thus, it is crucial to represent this co-variability in space and time (e.g. rectifier effect). Biospheric fluxes depend on meteorological conditions, but also anthropogenic emissions are influenced by meteorology (e.g. heating demand, traffic). Thus, modelling the fluxes, meteorology and atmospheric transport online in a coupled mode is desirable because it allows an optimal consistency between components and it also has the potential to transfer information from one component to another (e.g. atmospheric concentration to winds). For small-scale plumes, coupled data assimilation will be required to modify winds according to the observed plume. Otherwise, the MVS will be limited to plume imaging and mass-balance methods.

<u>EXAMPLES</u>: Coupled NWP models, Earth System Models (ESM)

- **OFFLINE MODELLING CAPABILITY**

As the focus is on trends on decadal scales, it is crucial to be able to run long simulations. The interactions between the different components can also create difficulties in the attribution and calibration of parameters. Therefore, it is also crucial to develop an offline modelling capability as a research tool and to have the potential of running long re-analysis simulations at lower cost. Offline transport models also offer the possibility to use long DA windows as atmospheric CO_2 and fluxes preserve the linearity assumption used in most DA methodologies. Offline models could also be used to perform controlled experiments for developing specific processes, e.g. calibration of model parameters.

EXAMPLES: Chemical Transport Models (CTMs), emission inventories, data-fusion products, offline land surface models, plume dispersion models

Evaluation of the different modelling and prior components is required to estimate their uncertainty for data assimilation purposes (see CHE D5.5, CHE D5.7), but also to assess priorities in the implementation of new model developments and new improved priors:

1. Sensitivity experiments to assess impact of priors, their temporal and spatial distribution and their interannual variability or model changes on the atmospheric signal
2. Model/product inter-comparison to benchmark new developments/priors
3. Evaluation with indirect observations (e.g. atmospheric observations)
4. Evaluation with direct observations (e.g. FLUXNET data)

3.2 Atmospheric transport

Atmospheric transport models act as operators that link the atmospheric CO_2 observations to the surface fluxes. Modelling atmospheric transport of CO_2 is not trivial. The high heterogeneity in the surface fluxes lead to complex horizontal and vertical gradients in the atmosphere. As CO_2 is a passive tracer, any small errors coming from meteorological input, numerical representation of transport processes or temporal spatial resolution can accumulate and become as large as the signal (e.g. atmospheric growth rate of around 2ppm). Many efforts have been devoted to transport inter-comparison studies (e.g. TransCom experiments by Rayner and Law, 1995; Law et al., 1996; Gurney et al., 2003; Patra et al., 2008, Law et al., 2008, Stephens et al., 2007; Karion et al. 2019). Despite the recent decrease in the spread between the transport models (Gaubert et al, 2019), transport still remains a major source of uncertainty in atmospheric CO_2 inversions (Basu et al., 2018).

There are two main approaches in the representation of transport from large-scale to local plumes:

- Offline transport (Chemical Transport Models): More flexibility in terms of options, but requires pre-processing of winds, in particular vertical wind is diagnosed through bottom-up mass balance. Yu et al. (2018) presents some of the limitations for the offline transport models.
- Online transport (Numerical Weather Prediction models extended with a module allowing flexible definition of (passive) tracers): Emphasis on consistency and high-resolution capability, instantaneous (time step) coupling, direct computation of winds

and parameterization of unresolved convective and turbulent mixing, as well as potential access to other ESM components such as land and ocean. Online models can consider feedbacks between components and offer the possibility of joint atmospheric composition - meteorology data assimilation (e.g. assimilation of CO_2 plume observations affecting simulated winds).

3.2.1 Eulerian transport models

Advection schemes

The horizontal and vertical transport that is resolved by Eulerian models is performed by advection schemes using wind information from an NWP model or NWP analysis. There are two main approaches:

- **Eulerian advection schemes** are commonly used by offline chemical transport models (e.g. CHIMERE, Gavete et al. 2012) They are also common in mesoscale NWP models such as WRF (Wang, 2009) or COSMO (Schneider and Bott, 2014) and global NWP models (e.g. nonhydrostatic finite-volume dynamical core IFS, Kühnline et al., 2019).The timesteps are restricted by maximum Courant–Friedrichs–Lewy (CFL) number criterion, implying short timesteps. They can be designed to conserve mass locally.
- **Semi-Lagrangian (SL) advection schemes** are commonly used in global NWP models and online tracer transport models e.g. IFS (Diamantakis, 2014), COSMO-GHG (Liu et al. 2017). They are very efficient for multi-species transport, with unconditional stability permitting long timesteps. However, they do not necessarily conserve mass locally, although solutions exist (Zerroukat, 2010). New versions of the scheme are being tested that are almost mass conservative (e.g. SL continuous mapping about the departure point in the IFS, see Malardel and Ricard, 2015).

Benchmarking:

Test for positive definiteness, shape preservation (preserving monotonicity and/or convexity), amplitude preservation (low degree of numerical diffusivity), mass conservation.

Unresolved transport: convection and turbulent mixing parameterisations

Small-scale transport associated with convective and turbulent mixing processes cannot be resolved by global and regional models running at horizontal resolutions of 10 to 1km and therefore requires a parameterization scheme:

- Convective transport is based on NWP parameterizations designed to transport water tracers, heat and momentum with a mass flux formulation. Transport models can compute the convective transport by calling the NWP convection schemes or by using the mass fluxes archived by NWP models (e.g. Feng et al. 2011). The role of the convection scheme depends on the model resolution.

- Shallow and deep convection are very efficient processes for the ventilation of tracer from the Planetary Boundary Layer (PBL) to the free troposphere (e.g. Yu et al., 2018, Belikov et al., 2013). Transient convection and PBL ventilation can be sensitive to temporal resolution of the model (Yu et al., 2018).
- Turbulent mixing distributes the anthropogenic emissions and natural fluxes from the surface throughout the PBL. Under stable conditions with low wind speeds, tracers remain trapped close to the surface. Modelling turbulent mixing under such conditions is very challenging (Sandu et al., 2013). Parameterizations of turbulent mixing can have a large impact on the wind speeds (Sandu et al. 2013), CO_2 concentrations (McGrath-Spangler et al., 2015) and plume dispersion from emission hotspots as shown by Large Eddy Simulations (LES, e.g. Gaudet et al., 2017). It is therefore crucial to improve the vertical profiles of winds and turbulence within the PBL to be able to model the plumes from hotspots (Karion et al. 2019).
- The coupling of shallow convection and turbulent mixing is an important aspect of NWP (water and energy cycles) and tracer transport (affecting long-range transport of tracers, including CO_2). ECMWF is addressing this coupling with the development of a more integrated physical parameterisation approach in the IFS which will be tested with CO_2 and other tracers.

Benchmarking: Use radon to assess convection and PBL mixing, model inter-comparisons and field experiments (e.g. GoAmazon model benchmark by Vila et al. 2019).

Lagrangian atmospheric dispersion models

Lagrangian models (LMs) track the movement of fluid parcels in their moving frame of reference (Lin et al., 2011). The most comprehensive LMs are Lagrangian Particle Dispersion Models (LPDMs) such as FLEXPART (Pisso et al. 2019) or STILT (Lin et al., 2003), which account for advective, turbulent and convective transport. LMs are known to create minimal numerical diffusion and thus are capable of preserving gradients in tracer concentration, for example in small-scale emission plumes. Additionally, Lagrangian integration is numerically stable, meaning that models can take bigger time steps. LPDMs can be run backward in time, allowing the computation of footprints (source-receptor sensitivities) as a basis for an analytical solution of the inversion problem. The downside is that LMs are computationally intensive when run for a large number of receptor points, which makes them less suited for the inversion of XCO_2 from satellites. LPDMs are offline models that run with meteorological output from both global (e.g. FLEXPART-IFS) and regional NWPs (e.g. WRF-STILT, FLEXPART-COSMO).

3.2.2 Evaluation

Transport model inter-comparison, use of multiple tracers to extract common errors based on direct evaluation of 4D tracer and wind fields with observations (e.g. CoMet field campaign).

3.3 Biogenic fluxes

There are three main approaches to estimate prior biogenic flux information based on statistical and biogeochemical models with differing degrees of model complexity and use of observations. They all have different advantages and disadvantages which are described in sub-sections below. However, all the methods rely on accurate input data, namely:

- mapping of land use (e.g. plant functional type and vegetation cover)
- satellite observations and ancillary Earth Observation (EO) data (e.g. albedo, FAPAR, LAI, vegetation indices, vegetation activity)
- meteorological data

Errors in the input data will lead to uncertainties and even biases in the biogenic fluxes, which could impact the estimation of anthropogenic emissions. Another key source of uncertainty in current biogenic models lies in the spatialization of parameters, which is usually done by Plant Functional Type (PFT). PFT makes models sensitive to PFT maps and it is an extremely poor way of spatializing biogeochemical parameters. Data-fusion product are less dependent on the fixed PFT structures. A systematic inter-comparison and assessment of the different approaches and the evaluation of the different products with FLUXNET data can help to benchmark the different approaches (section 4.2.4). While an ensemble of products could also be useful to provide an uncertainty estimate of the prior for the atmospheric inversion.

3.3.1 Data-fusion products

Data-driven products are designed to upscale the satellite and in situ observations of biogenic fluxes (NEE and GPP) using statistical regression models and predictors from other satellite products and NWP analysis. This approach allows a direct link with observations and non-prescribed relationships between fluxes and drivers/predictors unlike process-based models.

However, it can be challenging to estimate signals on such a wide range of different timescales (e.g. from hourly to annual/decadal) which might not be well represented by the predictors in the regression leading to underestimation of the seasonal cycle (Running et al., 2004) or the inter-annual variability (Jung et al., 2019).

There are multiple types of data-fusion products:

- NEE and GPP FLUXCOM product based on machine learning methods that upscale the eddy covariance measurements (see D3.2; Tramontana et al. 2016; Jung et al., 2017; Bodesheim et al., 2018; Walther et al., 2019). Ecosystem respiration is generally taken as the residual of NEE and GPP. The main advantage of FLUXCOM is that it makes direct use of in-situ FLUXNET data; makes it is easy to use different EO data streams (e.g. SIF); it is extremely data-adaptive compared to a fixed model structure; and it facilitates the derivation of the error covariance parameterizations as it is based on the in-situ FLUXNET data. The main disadvantages are the propagation of potential biases in the in-situ FLUXNET data, and the difficulty to make it operational and include it in a full FFDAS like system.

- GPP satellite products based on statistical models using solar-induced chlorophyll fluorescence (SIF) (Joiner et al., 2018). SIF is provided by many current and future satellites (including CO2M). It is considered an important constraint for the natural fluxes and thus it would help with the attribution of the CO_2 emissions/sinks.
- GPP satellite products based on simplified light use efficiency (LUE) models (Zhang et al., 2017).

3.3.2 Simplified models

Simplified diagnostic models use empirical parameters to represent response of plants to atmospheric drivers from NWP models and satellite data, and fixed look-up tables for the empirical parameters:

- The photosynthesis models are based on light-use-efficiency models. In CHE, such simplified models include the Vegetation Photosynthesis and Respiration Model (VPRM, Mahadevan et al. 2008, see D2.3), SDBM (Knorr and Heimann, 1995), and the A-gs model (Jacobs et al, 1996, 2007; Boussetta et al., 2013).
- The ecosystem respiration component is based on an empirical formulation (Boussetta et al., 2013).
- The advantage of such empirical models is that they have few parameters that can be optimized in a CCDAS approach (e.g. Kaminski et al., 2017). Due to their simplicity and low cost, they are also suited to run at high resolution (e.g. down to 1km for VPRM simulations in CHE, see D2.3) and in NRT (e.g. Agusti-Panareda et al., 2019). Because these models are usually diagnostic and they miss complex biochemical processes, they cannot be used in climate simulations.

3.3.3 Dynamic Global Vegetation Models (DGVMs)

DGVMs are complex biogeochemical models of terrestrial vegetation that are designed to represent the mechanistic processes of enzime kinetics associated with photosynthesis (Farquhar et al, 1980) and ecosystem respiration based the representation of carbon pools (e.g. JULES, LPJ-GUESS, NCAR-CLM4, ORCHIDEE, OCN, SDVGM, VEGAS, JSBACH, BETHY).

- The advantage of these DGVM is the inclusion of many biogeochemical processes and prognostic equation of the evolution of vegetation with time. Therefore, they can be used to run simulations over climate timescales (e.g., Sitch et al., 2008).
- The limitations include the high complexity of the DGVMs (Prentice et al., 2007) which include many highly uncertain processes and parameters leading to a large spread between models (e.g. Sitch et al., 2008, 2015).

3.3.4 Evaluation

Inter-comparison of FLUXCOM, SDBM, VPRM, A-gs (CTESSEL), ORCHIDEE, CASA-SiB, SiB4, etc with FLUXNET data. The caveat of this evaluation is the representation error, which could only be resolved if each model was run at the FLUXNET sites with the same observed forcing (see recommendations in section 5).

3.4 Anthropogenic emissions

Anthropogenic emissions grouped into a single source category provide a clear atmospheric signal and offer a simple option for modelling and attribution. However, a single category is no longer sufficient when considering the modelling of emissions, co-emission factors and uncertainties. Further detail can be gained by dividing emissions into sub-categories. For example, the daily temporal distribution of residential heating emissions can be modelled separately, using the heating degree day approach (e.g. Guevara *et al*., 2019a). Emissions from certain sectors (e.g. transport) are abundant in co-emitted species, which could provide additional information for sector specific attribution. The uncertainty associated with some sectors (e.g. energy) is significantly smaller than other sectors (e.g. solid waste incineration). For these reasons it is recommended that anthropogenic emissions be grouped into sectors, which can either be individually modelled and/or are representative of specific co-emitted species and specific uncertainties. The budget of each group must also be sufficiently large to generate a detectable modelled atmospheric signal, which is essential for source attribution. The following seven categories are recommended, super power stations, typical power stations, manufacturing/industry, residential combustion (settlements), aviation, non-aviation transport and other (Table 1).

3.4.1 Emission inventories based on Tier 1, Tier 2 and Tier 3 IPCC reporting

Anthropogenic emissions are typically derived with varying degrees of methodological complexity following IPCC (2006) guidelines. The estimated emissions per sector and country are the product of activity data (e.g. energy statistics) and an estimation of the quantity of emissions per unit activity (emission factor). The complexity by which the emissions are derived can be grouped into either tier-1 (basic), tier-2 (intermediate/technology-specific) or tier-3 (detailed/modelled) methodologies. Similarly, the spatial gridding of the estimated emissions can range in quality from tier-1 to tier-3 depending on the appropriateness of the spatial proxy being used for each sector, as reported by the EMEP/EEA (2016) guidelines. When comparing different emission inventories, studies sometimes show that the total amount of CO_2 emissions are quite similar but that strong discrepancies appear in their spatial distribution (e.g. allocation of CO_2 emissions related to residential heating or location of industries, Cai et al., 2018).

At a global scale the state-of-the-art emission inventory (Janssen-Maenhout et al. 2019, Choulga et al., 2020) adopts a tier-1/2 methodology; however more detailed information at the regional scale permits tier-2/3 methodologies to be adopted by European or national scale inventories (CHE D2.3). The methodology adopted by the selected inventory can inform uncertainty information.

Other tier-3 regional inventories are available for the USA (Vulcan, Gurney et al. (2009), and HESTIA, Gurney et al., 2019), Canada, South America and China (e.g. CHRED, Cai et al, 2018). New tools are being developed to make use of this mosaic of regional inventories by combining them with global inventories like EDGAR at the global scale and processing them for use in atmospheric transport models (e.g. HEMCO by Keller et al., 2014 and HERMES by Guevara et al., 2019a). An example of such a merged mosaic inventory is HTAPv2.2 (Janssens-Maenhout et al., 2015). However, as inventories may differ in e.g., sector definitions, distribution proxies, etc. specific attention is needed to assure consistency across the domain.

Benchmarking:

Comparison of EDGAR and TNO inventories and links to UNFCCC over European domain and with non-European tier-3 inventories if available.

Table 1 Anthropogenic CO_2 emission sectors, their global budget and co-emitters (see Table 1 from Janssen-Maenhout et al. (2019) for a description of the EDGAR sectors).

ECMWF group	EDGAR sector	IPCC2006 activity	Global budget[1]		Co-emitters		
			Total Mton	Uncertainty %	NOx	CO	PM2.5
ENERGY_S	ENE	1.A.1.a (subset)	897	-7/+2	✓	x[2]	
ENERGY_A	ENE	1.A.1.a (rest)	11’672	-7/+7	✓	X[2]	
	SWD-INC	4.C	137	-40/+40	✓	✓	✓
MANUFACTURING	IND	1.A.2	7’329	-7/+7	✓	✓	✓
	IRO	2.C.1, 2.C.2	234	-31/+31			
	NFE	2.C.3, 2.C.4, 2.C.5, 2.C.6, 2.C.7	91	-43/+72			
	NEU	2.D.1, 2.D.2, 2.D.4	25	-58/+127			
	NMM	2.A.1, 2.A.2, 2.A.3, 2.A.4	1’749	-42/+70			
	CHE	2.B.1, 2.B.2, 2.B.3, 2.B.4, 2.B.5, 2.B.6, 2.B.8	677	-50/+82			
SETTLEMENTS	RCO	1.A.4, 1.A.5.a, 1.A.5.b.i, 1.A.5.b.ii	3’323	-11/+11	x[3]	✓	✓
AVIATION	TNR-Aviation-CRS	1.A.3.a_CRS	412	-21/+70	✓	x[4]	

[1] CO_2 emission budgets are based on the global emission maps used in the CHE project

[2] Power plants show high energy efficiency of the combustion at high temperature. Therefore they emit little CO but do they emit NOx. However, the de-NOx – de-SOx abatement can show high efficiencies in the range of 96-99%.

[3] Residential heating systems can vary, but if locally implemented, a boiler at home is not showing the same high temperature combustion as the power plants and so can have lower efficiency combustion with emission of CO and less NOx

[4] The turbines of airplanes are typically having a higher temperature combustion, with rather NOx emissions than CO

	TNR-Aviation-CDS	1.A.3.a_CDS	306	-14/+47	✓	x	
	TNR-Aviation-LTO	1.A.3.a_LTO	98	-12/+38	✓	x	
TRANSPORT	TRO	1.A.3.b	5’531	-4/+4	✓	✓	✓
	TNR-Ship	1.A.3.d	819	-35/+49	✓	✓	✓
	TNR-Other	1.A.3.c, 1.A.3.e	255	-29/+98	✓	✓	✓
OTHER	REF-TRF	1.A.1.b, 1.A.1.c, 1.A.5.b.iii, 1.B.1.c, 1.B.2.a.iii.4, 1.B.2.a.iii.6, 1.B.2.b.iii.3	1’918	-32/+144		✓	✓

3.4.2 Emission vertical profiles

Local sources from power plants and industrial facilities are not emitted at surface but from chimney stacks with heights from 100 to 200m above the ground and at high temperatures their plumes can rise higher (Brunner et al., 2019). Emission vertical profiles and plume rise models are regularly used in regional air quality models (e.g. Bieser et al., 2011; Guevara et al., 2014) and they have been shown to have a significant impact on surface CO2 and XCO2 over Europe (Brunner et al., 2019). The tracer injection heights are usually computed with a plume rise model and input stack parameters like stack height, effluent temperature, and volume flux. This information is not available for the point sources over the globe and therefore some assumptions would be required to use the plume rise model on a global domain.

Emitting from a point source is not the same as emitting over a model grid cell of 10kmx10km as used currently by the IFS. Further testing of the plume rise model needs to be done to understand the impact of horizontal and vertical resolution on the most effective vertical allocation of the point source.

Benchmarking:

Assessment of impact of sector dependent vertical profiles on atmospheric CO_2 variability (e.g. Brunner et al. 2019).

3.4.3 Emission temporal profiles

Accurate modelling of anthropogenic emissions requires detailed high-resolution temporal profiles, which are often unavailable. Offline emissions are typically constant at annual (EDGAR v4.3.2, Janssen-Maenhout et al., 2019) or monthly (EDGAR v4.2FT2010) timescales. Higher temporal frequency can be included online using prescribed functions for weekly and hourly timescales (e.g. biomass burning diurnal cycle implemented in CAMS). CHE regional models apply such fixed temporal profiles over Europe (Liu et al., 2017). Global models generally do not use such high frequency profiles because it can also introduce high uncertainty, as this variability is largely dependent on country and/or climatic zones. Some generic profiles have been derived for specific regional inventories (e.g. Nassar et al., 2013, Denier van der Gon et al, 2011, Pouliot et al, 2012) and CAMS is now producing global and regional gridded temporal profiles for monthly, weekly, daily and hourly timescales for several species (e.g. NO_2, CO, PM2.5, CO_2, CH_4) and sectors based on activity data from a range of countries. For CO_2 gridded temporal profiles for energy, transport and residential heating are available. Given the high I/O requirements of using high temporal resolution emissions for the different sectors, the current strategy is to use monthly emission datasets and integrate the higher resolution temporal profiles (i.e. weekly, daily and hourly variations) in the model.

Benchmarking:

Assessment of impact of fixed emission temporal profiles on atmospheric CO_2 variability (e.g. Liu et al. 2017).

3.4.4 Modelling fossil fuel emissions (FFDAS approach)

A fossil fuel data assimilation system offers the potential to constrain the spatial distribution of anthropogenic emissions in NRT. National statistics or nightlight observations can be used to constrain emissions based on variables such as population density, economic activity or traffic activity data. Models such as these (e.g. Rayner et al., 2010) can be used to either inform prior emissions for use in atmospheric models or they can be combined with atmospheric models and atmospheric observations of CO_2 for parameter optimisation, which can provide posterior flux information.

For certain sectors, such as residential heating, temporal profiles can be derived online using temperature values from the model atmospheric fields (e.g. Matthias et al., 2018; Guevara et al., 2019b). These can be used to update emissions at high temporal frequency. Atmospheric variables could also be used to inform energy emissions, through variability in demand. Online emissions need to be carefully configured to ensure the global budget in the model is conserved, this may require the model to be run in reanalysis mode using historical meteorological data. The advantage of this approach is that it provides a very efficient spatial and temporal disaggregation of the emission statistics.

Future developments should focus on a synergy between modelling trace gas emissions and urban schemes for numerical weather prediction (NWP). Urban schemes for NWP have varying degrees of complexity and can be considered as either slab tiles, single layer canopies or multi-layer canopies. The more basic slab (e.g. Best, 2005) and single layer canopy models (e.g. Porson *et al* 2010) could be used on a global scale using only a few parameters, which are currently available from providers (e.g. urban fraction). These produce surface temperatures, which would inform a residential emissions model. More complex emission models which require more variables may be dependent on complex multi-layer urban canopy models (e.g. Masson *et al*., 2000). Efforts have already begun to combine these local scale urban schemes with a CO_2 emission model (Goret *et al*., 2019).

Benchmarking:

Assessment of impact of residential heating profiles in CHE nature run on atmospheric CO_2 variability.

3.4.5 Co-emitted species and other tracers for source/sink attribution

Combustion processes, which are an important anthropogenic source for CO_2, co-emit chemically reactive species that play an important role in the chemistry of the atmosphere. Because of the rapid chemical conversions and removal processes, the spatio-temporal gradients of these species are often more pronounced than the gradients of CO_2, and they are much less influenced by biogenic activity. These two aspects make the reactive species good markers for anthropogenic emissions from different sectors (listed in Table 1). Important examples of the co-emitted species are nitrogen oxide (NO), nitrogen dioxide (NO_2), carbon monoxide (CO) and sulphur dioxide (SO_2). Most of these species are observed with the air quality in-situ network at the surface and with satellite instruments. In particular, NO_2 can be monitored at a high spatial (e.g. TROPOMI, Eskes et al., 2019) and temporal resolution (e.g.

Sentinel 4) with current or planned satellite missions. Another approach for the fossil fuel attribution is to use the radioactive isotope of carbon ($^{14}CO2$) from in situ observations (CHE D4.1) which is depleted in fossil fuels, or Atmospheric Potential Oxygen (APO) which is based on the variation of oxygen to nitrogen ratio associated with fossil fuel combustion (see CHE D4.1 and CHE D4.3 for further details).

- CO and NOx are co-emitted by combustion processes (e.g. energy production, transport, residential heating) and therefore can provide information on attribution of specific sectors (see Table 1, CHE D4.3). We require prior information of co-emitted species in terms of emissions, atmospheric sink associated with chemistry, atmospheric initial conditions and/or emission factors (depending on the definition of the control vector in data assimilation). Emission factors depend on sector and fuel type (for CO_2) and on technology (for NOx, CO, PM2.5) and differ amongst regions and even within one country. Therefore, they are highly uncertain. The key question is whether regional spatial averages of sectoral emission factors are well characterized or whether they are chaotic (i.e. not stable) like emitter-to-emitter variations. The activity data show large temporal and spatial variability and therefore they can become highly uncertain. The initial and boundary conditions are available from the CAMS re-analysis (Inness et al., 2019).
- Radiocarbon is potentially a very useful marker to trace fossil fuel emissions. However, it is a complex tracer to model (see CHE D4.3) with limited availability of observations (CHE D5.1). This requires representation of sources (cosmogenic and nuclear power), as well as the adaptation of the atmospheric CO_2 and anthropogenic emissions (fossil fuel and bio fuels), ocean fluxes, biomass burning and biogenic CO_2 flux model in order to represent the isotope fractionation associated with all the processes (Wang, 2016; Wang et al., 2018). Initial conditions and boundary conditions for regional models are also required. In CHE they have been provided by the LMDZ simulation of Wang (2016).
- Atmospheric Potential Oxygen (APO) is also a complex tracer to model with limited availability of observations (see CHE D4.3), requiring information on: O_2 consumption flux from anthropogenic emissions (fossil fuel, biofuel); the O_2:CO_2 ratio of terrestrial biospheric exchange (per biome and soil type); gridded ocean CO_2, O_2 and N_2 fluxes; biomass burning O_2/CO_2 ratios (based on CO:CO_2 ratios); and photochemical CO and CH_4 oxidation from reaction with OH (associated with net loss of atmospheric O_2). Finally, atmospheric initial and boundary conditions are also required as input. In CHE, these have been obtained from the Jena Carboscope inversions (Rödenbeck et al, 2013).
- Carbonyl Sulfide (COS) is a tracer that can be used to constrain gross primary productivity associated with photosynthesis by vegetation (Launois et al., 2015). The observations available are described in D5.1. The model requirements comprise: atmospheric sink, its ocean emissions, its soil fluxes, its anthropogenic emissions, its biomass burning emissions and the leaf relative uptake ratio of COS to CO_2 fluxes.

3.4.6 Evaluation

- Inter-comparison of emission data sets (e.g. EDGAR, TNO)
- Input of atmospheric modeling on the sensitivity of the used spatial distribution, the temporal profiles
- Consistency between emission fields of CO_2 and of co-emitted species
- Check on the sub-regional detailed inventory and the same region of the global inventory – the total is constrained at country level.
- Explore information in additional tracers like C14, APO.

3.5 Biomass burning emissions

Fire is an essential component of the Earth system contributing significant amounts of greenhouse gases, trace gases and particulate matter to the atmosphere. Satellite measurements of global fires provide information on the location and timing of active fires and can be used to estimate emissions using observations of either the burnt area (BA) or fire radiative power (FRP). In both cases these observations are used to estimate the dry matter consumed by fire which is used in the emission estimation based on vegetation type and emission factors derived from laboratory and field studies. Currently available datasets of fire emissions use both burned area (e.g., Global Fire Emissions Database, GFED) and FRP (e.g., Global Fire Assimilation System, GFAS; Fire INventory from NCAR, FINN). Total estimated emissions are generally consistent between the two approaches and the choice of which method to use depends on the application: the BA approach provides information on extent of burning in addition to the emissions but is not available in NRT; the FRP approach is available in NRT and is more suitable for operational applications. Improvements in estimating global fire emissions are anticipated in the near future through the use of real-time satellite observations from geostationary and LEO orbits, improvements in vegetation/land cover maps, and improved emission factors from laboratory and field studies.

3.6 Ocean fluxes

Ocean CO_2 fluxes can also be estimated using data-fusion methods with pCO_2-based products (e.g. Takahashi et al., 2009) or global ocean biogeochemistry models (GOBMs):

- The GOBM represent the physical, biological and chemical processes that control the CO2 concentration in the ocean (e.g. CCSM-BEC, Doney et al. (2009); MICOM-HAMOCC, Schwinger et al., 2016; MITgcm-RecoM2, Hauck et al., 2016; MPIOM-HAMOCC, Mauritsen et al., 2019; NEMO-PISCES (CNRM), Berthet et al., 2019; NEMO-PISCES (IPSL), Aumont and Bopp, 2006; NEMO-PlankTOM5, Buitenhuis et al., 2010). Like the DGVMs they require inputs for the atmospheric forcing (e.g. from NWP re-analysis). They are complex costly models, with prognostic skill to run in climate simulations.
- Data-based products are designed to exploit all the available pCO_2 observations over the ocean from the SOCAT database using either neural networks (e.g. Landschützer et al.,2015) or simple parameterizations of the ocean mixed layer (e.g. Rödenbeck et al., 2014).

A comparison between the annual ocean CO_2 sink from GOBM and pCO_2 flux products shows there is consistency in the underlying variability (Le Quéré et al., 2018, Friedlingstein et al., 2019).

3.7 Atmospheric chemistry

Modelling combustion short-lived species (CO and NO_x) to infer CO_2 sources requires the simulation of the chemical conversions, removal processes and the emissions in the atmosphere. Of particular importance are the fast chemical conversions between the emitted but very-short lived NO and the longer lived but well-observed NO_2 in the presence of other chemical species such as ozone and OH. Chemical schemes comprising of 50-120 species have been integrated in the IFS as part of the GEMS, MACC and CAMS projects (Flemming et al, 2015, Huijnen, et al. 2019). The IFS in CAMS configuration is used operationally to forecast atmospheric composition and to assimilate satellite retrievals of NO_2, CO, ozone, SO_2 and Aerosol Optical Depth (Inness et al. 2019).

But, the computational cost of the chemical schemes is considerable, which may require the development of computationally affordable but still adequate versions of the chemistry scheme for the application in CHE. The development of simplified schemes is already a growing research focus in CAMS because affordable schemes are intended to be used to better represent atmospheric chemistry in the tangent-linear and adjoint formulation of the IFS applied in the 4DVAR data assimilation approach. For example, the development of a surrogate model for chemistry using machine learning algorithms will be developed as part of a NASA project run by University of Colorado in collaboration with ECMWF.

4 Progress in integration and recent developments

The integration of the different model and prior components of the CO2MVS depicted in Figure 1 has been tested in the context of various CHE nature run simulations of CO_2 and co-emitters (CHE D2.1, D2.2, D2.4, D2.6, D2.8). This integration relies greatly on the consistent mapping of the land surface cover which provides inputs to the inventories, the numerical weather prediction model and the vegetation model (as indicated by the arrows in Figure 1). These and other aspects that play an important role in the realism of the simulations are presented here to illustrate the progress and challenges that will need to be addressed in the implementation of the CO2MVS during the follow-on project CoCO2.

The coupling of the different components in the framework of Earth System Modelling depicted in Figure 2 is still ongoing. The CO2MVS will benefit from the integration with NWP in order to improve the accuracy of tracer transport. Section 4.1 presents recent developments in the tracer advection scheme of the Integrated Forecasting System at ECMWF on which the CO2M observation operator of the global CO2 MVS will be based. Highlights of the multi-scale and multi-species simulations focusing on plumes from emission hotspots are provided in section 4.2, emphasizing the benefits and challenges of using co-emitted species, as well as temporal and vertical variability of emissions. Section 4.3 presents the new developments of the urban model in the IFS which will allow to compute residential heating emissions online with high temporal and spatial resolution. The importance of the biogenic fluxes in explaining the atmospheric CO_2 signal and the mapping activities affecting the biogenic fluxes are presented in section 4.4. The integration of specific emission sectors such as residential heating and biogenic fluxes in the ESM will improve the consistency between emissions and sinks of CO_2 and atmospheric transport in the CO2MVS. This will result in a better representation of the rectifier effect (Denning et al., 1999, Liu et al., 2017) and therefore it will make the modelling more realistic.

4.1 Numerical schemes and parameterisation of atmospheric tracer transport

The atmospheric inversion system in the MVS relies on the accurate representation of atmospheric tracer transport as the operator that translates the information of observed atmospheric concentrations to natural surface fluxes and anthropogenic emissions. In particular, numerical errors in the transport model, including tracer and total air mass conservation (Agusti-Panareda et al., 2017), numerical diffusion (Eastham and Jacob, 2017) and parameterization of sub-grid scale processes (Yu et al., 2018) affect all tracer transport models to various degrees, potentially leading to regional biases that are difficult to diagnose and will impair the reliability of the inversion results. Therefore, the evaluation of numerical and physical parameterisation schemes in transport models remain a priority. For example, the IFS tracer transport is known to be very efficient and robust, but suffers from mass conservation errors which are addressed in the CAMS atmospheric composition analysis and forecasting system with a mass fixer (Diamantakis and Agusti-Panareda et al., 2017). An alternative interpolation method for the standard semi-Lagrangian advection scheme (COMAD, Malardel et al., 2015) that introduces the concept of cell-averaging and improves its conservation properties will be tested and further adapted for CO_2 and other tracers in the IFS. Figure 3 shows some preliminary results of the COMAD advection in the IFS which leads to a smaller XCO_2 correction by the mass fixer than the standard semi-Lagrangian advection.

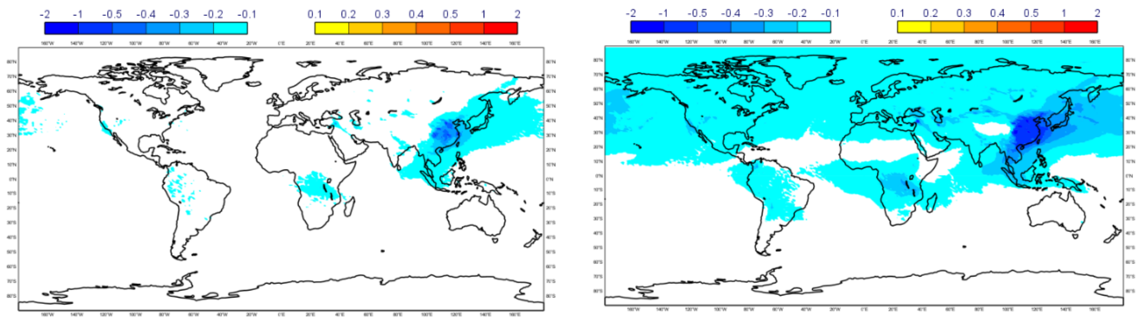

Figure 3 Accumulated XCO_2 mass fixer correction [ppm] for the new COMAD semi-Lagrangian advection scheme (left) compared to the standard scheme used operationally in CAMS CO_2 analysis and forecasts and in the CHE nature runs (right) after one month of simulation in January 2015.

Atmospheric boundary layer mixing is another aspect of transport models that urgently requires further investigation. Most inversion systems are only able to assimilate observations near the surface during the afternoon when well-mixed conditions are prevalent, because of the large uncertainty of turbulent mixing under stable conditions. Using tracers like radon (Williams et al., 2011) which have a distinct concentration in the boundary layer and free troposphere can help to diagnose transport errors near the surface (Chambers et al., 2015). The correlation between radon concentrations measured at the ICOS sites and the boundary layer height (Figure 4) will be further exploited to investigate the transport model error in the boundary layer in the CoCO2 nature runs.

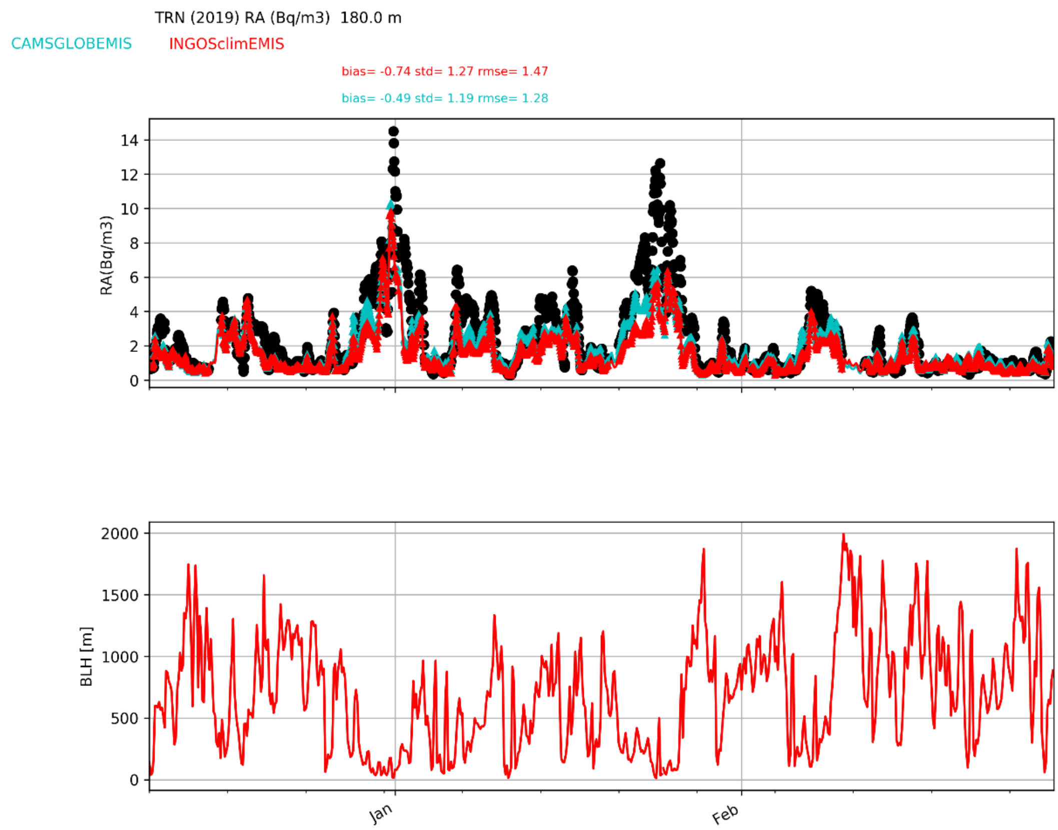

Figure 4 IFS simulation of hourly radon (222Rn) concentrations [Bq/m3] and atmospheric Boundary Layer Height (BLH) [m] at Trainou (France) (Schmidt et al., 2014) ICOS-Atmosphere Thematic Centre station for the period from 1 December 2019 to 28 February 2020. Radon observations [Bq/m3] are shown as black circles and simulated values are shown with coloured circles based on two different emission datasets: a climatology from Karstens et al. 2015 (red circles) and zonally averaged emissions used in the CAMS operational forecast (cyan circles).

4.2 Plume simulations with co-emitted species

Power plants are an important source of CO_2. In Europe, approximately 50% of CO_2 is emitted from power plants and other point sources through stacks (Brunner et al., 2019). As illustrated in Figure 5 showing simulated column mean dry air mole fractions XCO_2 over Germany on 2 November 2015, these point sources generate a large number of plumes with pronounced local enhancements in XCO_2 that can potentially be imaged by the CO2M mission. An important question is thus, how well such plumes can be simulated by atmospheric transport models and what resolution is required to properly represent their main characteristics.

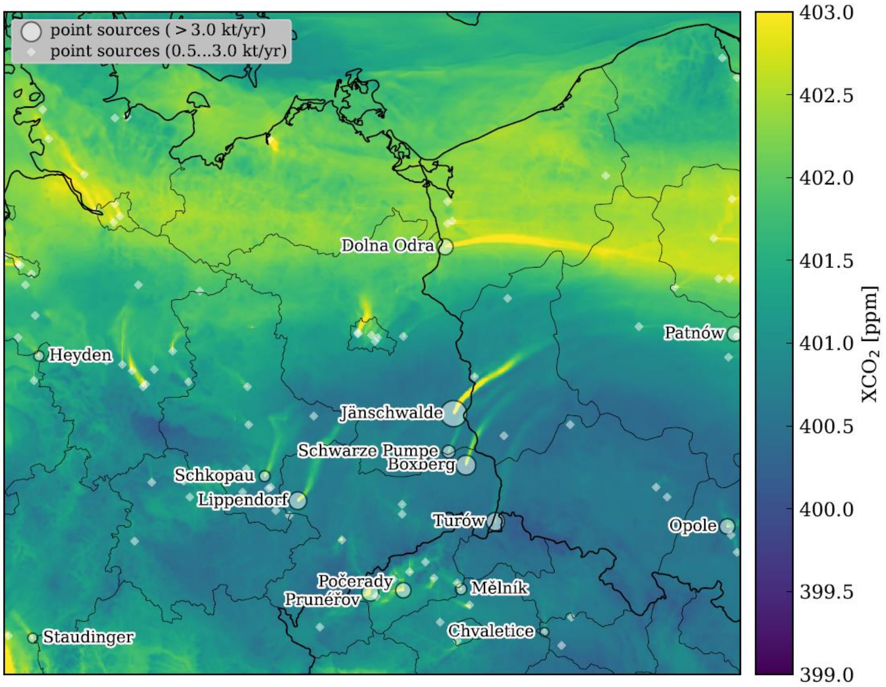

Figure 5 Column-averaged dry air mole fractions XCO_2 on 2 Nov 2015 over a domain covering parts of Germany, Poland and the Czech Republic as simulated by COSMO-GHG at 1 km horizontal resolution. The 15 largest point sources in the domain are labelled. Weaker point sources are marked by diamonds.

In order to investigate the impact of model resolution, simulations from different models operating at different resolutions were compared:

- CHE Tier 1 global nature run, IFS model, 9 km horizontal resolution, year 2015
- CHE European nature run, COSMO-GHG model, 5 km resolution, year 2015
- CHE Berlin nature run, COSMO-GHG model, 1 km resolution, year 2015
- COSMO-GHG simulations of selected plumes of power plants Belchatow (Poland) and Jänschwalde (Germany), 1 km resolution, few days in 2018
- EULAG LES simulations of Belchatow plumes, 200 m resolution, days in 2018

Figure 6 presents an example of the representation of power plant plumes in eastern Germany in different CHE nature runs. The figure presents a snapshot of XCO_2 on 9 March 2015 at 09:00 UTC. In the COSMO-GHG simulation at 1 km resolution, the three plumes are very pronounced with amplitudes of up to 4 ppm above background. They are still easily visible in the COSMO-GHG simulation at 5 km resolution but the individual plumes are more dispersed and start to overlap. In the global Tier-1 simulation at 9 km resolution, the individual plumes are hard to distinguish, but rather a single broad plume with a maximum amplitude of about 1 ppm emanates from the area of the power plants. The coarser resolution thus leads to a strong dilution, which will make it more difficult to identify the plumes against variations in the background and to discriminate individual sources, if they are located close to each other, which is quite a typical situation for power plants (see Fig. 5).

Figure 6 also illustrates the importance of the underlying emission inventory and of the vertical placement of the emissions from power plants. While plume rise was explicitly accounted for in the COSMO-GHG simulations, CO_2 was emitted at the surface in the CHE Tier-1 simulation.

Because of strong vertical wind shear on this day, the plume was therefore advected into a different direction in the IFS model. When CO_2 was also emitted at the surface in the COSMO-GHG model, the plume was transported in the same direction as in the IFS model (lower right panel), demonstrating that these differences were not due to different meteorology but due to the vertical placement of the emissions.

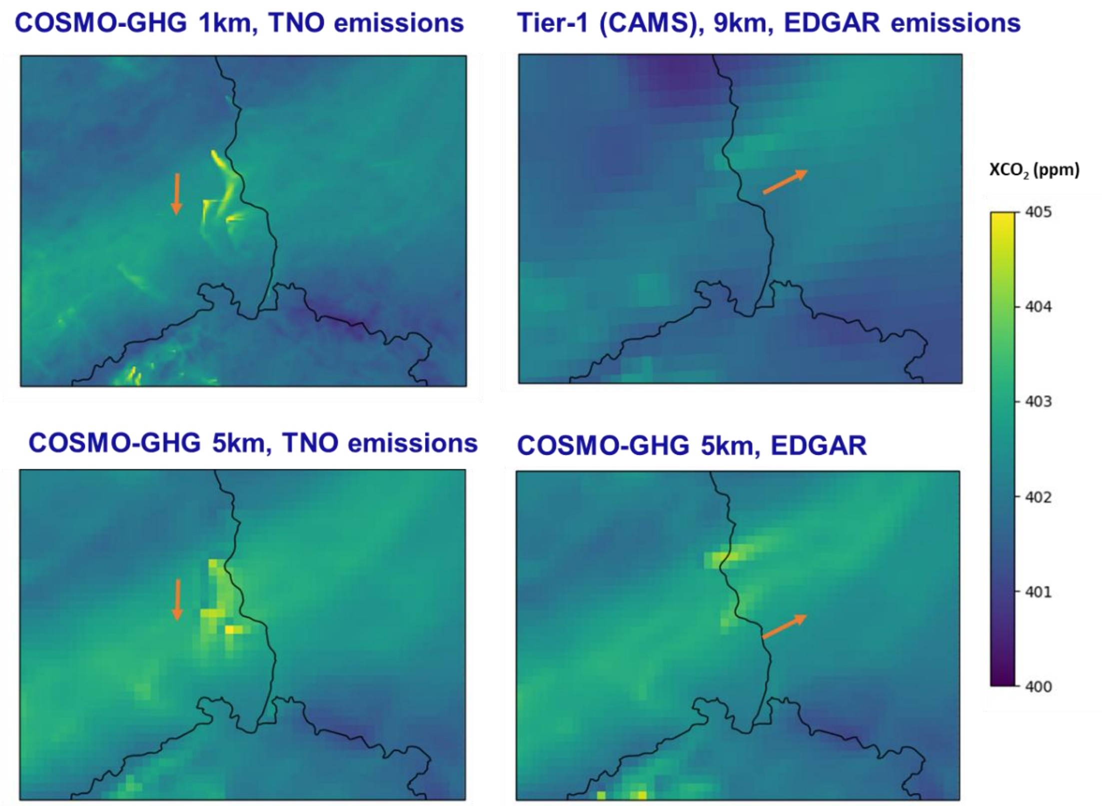

Figure 6 Column-averaged dry air mole fractions XCO_2 on 9 Mar 2015 09:00 UTC over a domain in eastern Germany with three coal-fired power plants (Jänschwalde, Schwarze Pumpe, Boxberg) simulated by different models at different resolutions. Left: COSMO-GHG at 1 km and 5 km horizontal resolution with emissions from TNO inventory and accounting for vertical plume rise. Right: IFS Tier-1 simulation at 9 km resolution and COSMO-GHG simulation at 5 km resolution using the EDGAR inventory and emitting CO_2 only at the surface. Red arrows indicate the direction of propagation of the plume.

Even higher resolution simulations (at 200 m horizontal grid spacing) were conducted with the Large Eddy Simulation (LES) model EULAG, in order to provide a reference for coarser models. Figure 7 shows the XCO_2 plume of the power plant Belchatow, the largest ignite power plant in Europe, simulated by EULAG for 7 June 2018, 13:00 UTC. The individual panels show the simulation at the original and downgraded to lower resolutions. The simulation was driven at the lateral boundaries by meteorological output of a 1 km simulation of the COSMO-GHG model in order to provide a realistic larger scale forcing. The meteorological situation was sunny and convective leading to a highly turbulent plume strongly deviating from a classical Gaussian shape as seen in the figure. At lower resolution, the plume becomes more Gaussian, but pockets of higher and lower concentrations caused by the turbulence are still visible at the resolution of CO2M (~2 km) and even at 4.2 km resolution.

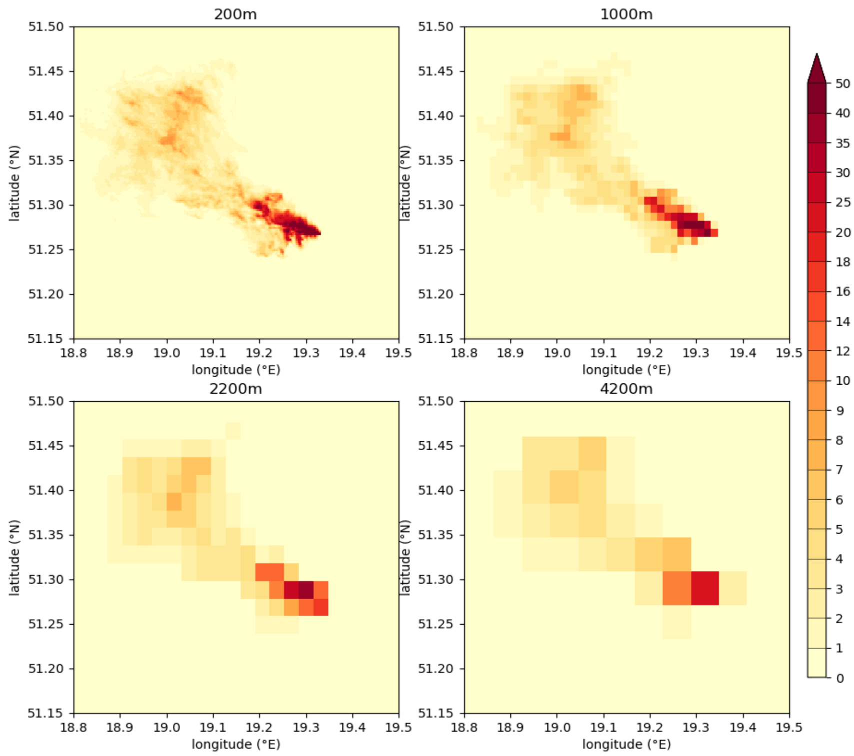

Figure 7 Column-averaged dry air mole fractions XCO_2 on 7 Jun 2018 13:00 UTC as simulated by the EULAG LES model. The panels show the simulation at the original resolution (top left) and downgraded (averaged) to lower resolutions of 1 km, 2.2 km and 4.2 km.

In order to assess the realism of the simulations, the plumes simulated by EULAG and the COSMO-GHG (1 km) model were compared with aircraft in situ and remote sensing observations from the CoMet measurement campaign collected on 7 Jun 2018 (Fiehn et al., 2020). Measurements were collected from three aircraft transecting or overflying the plume multiple times at different distances from the power plant. An example of the comparison with total column XCO_2 as measured by the MAMAP spectrometer of the University of Bremen is presented in Figure 8. The figure suggests that the EULAG model realistically simulates the amplitude and fine-scale structure of the plume, while it is smoothed out too strongly in the COSMO-GHG model. Overall, the comparisons with the observations for this case and for another case with observations of the Jänschwalde plume, lead to the following conclusions:

- The models quite realistically represent the fine-scale structure and turbulent nature of the plumes
- Due to the stochastic nature of turbulence, it is impossible for a model to exactly capture the plume structure at a given instant in time. Therefore, models need to be assessed for their ability to represent statistical properties of a plume such as mean plume width and amplitude as a function of distance or frequency distributions of the CO_2 enhancements.
- The Belchatow and Jänschwalde plumes were observed under different meteorological conditions that produced very different plumes: A highly complex, turbulent plume in the case of Belchatow, a smooth Gaussian-shaped plume in case of Jänschwalde. Less turbulent situations are easier to simulate.
- The COSMO-GHG model tends to overestimate plume dispersion: With increasing distance from the source, simulated plume widths tend to be larger than observed

- Accounting for plume rise is highly relevant: The in-situ measurements suggest that the plumes extended to about 1600 m (Belchatow) and 1000 m (Jänschwalde) already at short distances (~10 km) from the source. The observed plumes could only be reproduced realistically when accounting for plume rise.

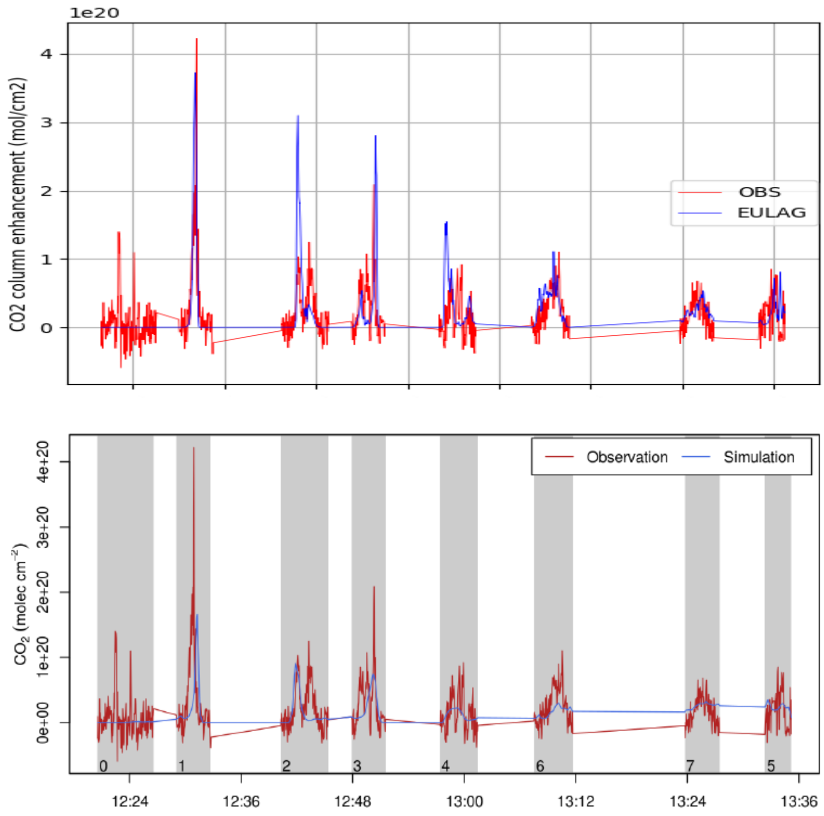

Figure 8 Comparison of simulated column-averaged dry air mole fractions XCO$_2$ of the Belchatow plume on 7 Jun 2018 with measurements of the airborne MAMAP spectrometer of the University of Bremen. Top: EULAG LES model. Bottom: COSMO-GHG model. Overpasses over the plume are numbered 1-7 corresponding to increasing distances from the source between 2 km (transect 1) and 23.8 km (transect 7).

The value of additional satellite observations of trace gases like NO_2 and CO emitted by combustion processes for the quantification of CO_2 emissions from cities and power plants was studied in the ESA project SMARTCARB. In particular NO_2 was found to be highly beneficial for several reasons: (i) NO_2 has low background concentrations due to its short lifetime, so that plumes can easily be discriminated against variations in the background. (ii) Biospheric sources of NO_x are low compared to anthropogenic emissions. (iii) NO_2 can be measured from satellites with comparatively high precision, as demonstrated by recent satellite missions such as TROPOMI.

As shown in Figure 9, NO_2 plumes can therefore be more easily detected in satellite observations than CO_2 plumes. The figure is based on synthetic satellite observations of CO_2 and NO_2 generated from a 1 km x 1 km resolution COSMO-GHG simulation and applying realistic instrument noise levels. It shows the plume of the city of Berlin on 21 April 2015. The true CO_2 and NO_2 plumes as determined from a tracer representing only emissions of Berlin are outlined by black solid and dashed lines, respectively. A plume detection algorithm was then applied to the noise images to identify pixels with values significantly above background (Kuhlmann et al. 2019). The figure shows that a much larger proportion of the plume can be detected from the NO_2 observations compared to CO_2. As shown in Kuhlmann et al. (2020), additional NO_2 observations allow quantifying CO_2 emissions from a larger number of plumes and with much better accuracy. NO_2 was simulated here in a highly simplified way with a constant decay time of 4 hours. Full chemistry simulations are necessary to capture the complex photochemical processing of NO_2 in the plumes. It should be investigated in a future project how well a simplified NO_2 tracer agrees with a full chemistry tracer.

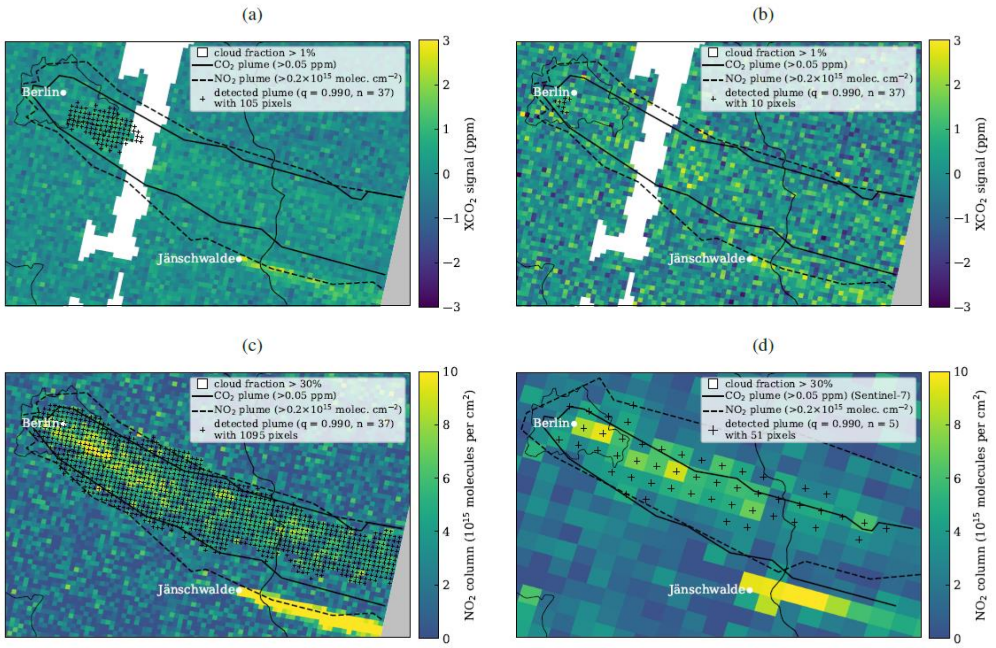

Figure 9 Example of plume detection in (simulated) CO_2 and NO_2 satellite observations on 21 April 2015. Significant pixels detected by a plume detection algorithm are highlighted as black crosses. The outlines of the true CO_2 and NO_2 plumes based on Berlin emission tracers are overlaid as solid and dashed lines, respectively. (a) Low-noise CO_2 instrument. (b) high-noise CO_2 instrument. (c) High-noise NO_2 instrument on the CO2M satellite. (d) NO_2 instrument on Sentinel-5 (from Kuhlmann et al., 2019).

4.3 Urban model

New developments of a simple urban model in the Integrated Forecasting System at ECMWF will result in a more accurate representation of the energy, water and carbon fluxes over urban areas. The introduction of an urban tile within the IFS has begun with initial testing using the single column model (SCM) and the global offline surface model (GOSM). The advantages of the new tile are expected to be two-fold, firstly to provide improved NWP scores and secondly to introduce an online residential emissions model. The developments are expected to follow a similar path to the existing online vegetation model, which provides both NWP relevant information and online biogenic CO_2 fluxes. The CO_2 residential emissions model will be largely based on Guevera et al. (2013).

The aim is to implement a single layer urban model within the IFS, which uses mapped parameters to derive surface energy and hydrology fluxes. The model considers radiation using an infinite canyon assumption, accounting for shadowing, which is dependent on urban parameters and the solar zenith angle. The surface roughness is generated using building properties and information on canyon geometry, removing any concept of canyon orientation. Thermal and hydrological properties are also defined by several urban parameters, accounting for not only land-atmosphere exchange but also sub-surface exchanges of both heat and water. The scheme consists of both time varying (e.g. albedo based on solar zenith angle) and constant variables (e.g thermal heat capacity of a building). It is optimised using a Gauss-Newton non-linear least-square approximation to derive parameter values in the SCM, and results are shown in Figure 10, taken from an upcoming study (McNorton *et al.* in prep). Early results show improved model forecast over urban areas with future work aimed at implementing the scheme operationally. The urban scheme is currently being used in a global surface-only version of the IFS, with results showing the expected enhancement in night-time 2m temperature (Figure 11).

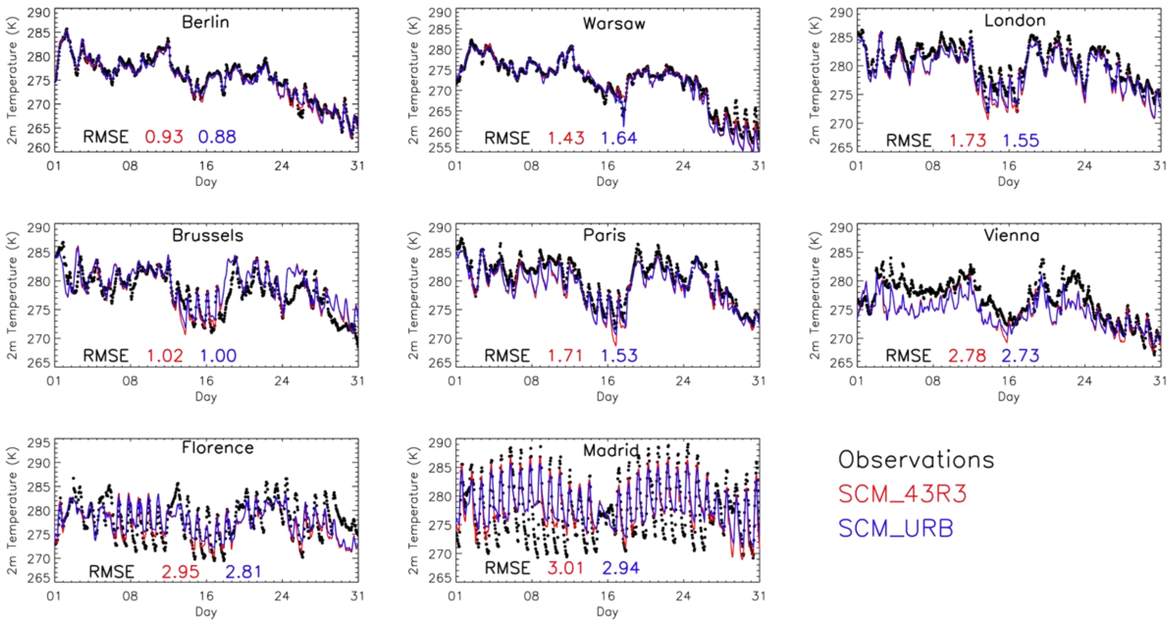

Figure 10 Hourly observed 2m temperature taken from 8 urban sites for January 2012 (black circles). Also shown are IFS single column model results using both a control (red) and the urban scheme (blue). Values indicate the RMSE values for comparison of model and observations.

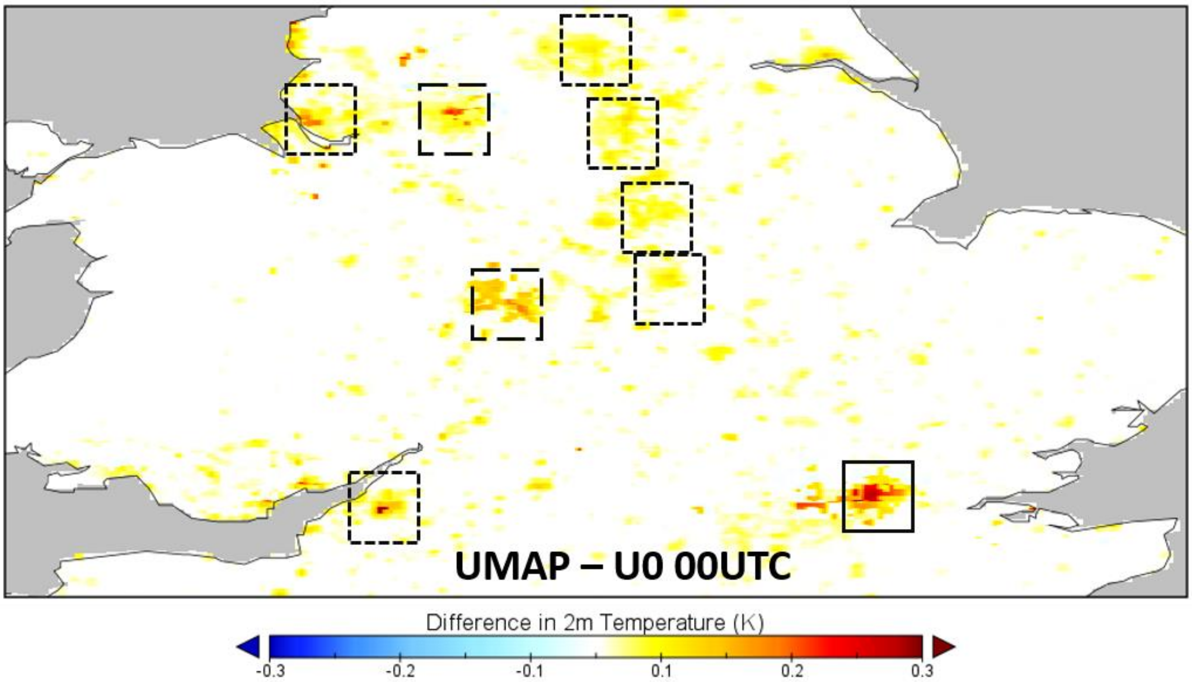

Figure 11 The difference in modelled average 2m temperature over Southern UK between the urban scheme and the control for 00 UTC during January 2019. Conurbations larger than 1,000 km2 (solid), 500 km2 (dashed) and 100 km2 (dotted) are denoted with boxes.

Sentinel-5 (from Kuhlmann et al., 2019).

4.4 Biogenic CO2 fluxes

Biogenic fluxes of CO_2 are very important to explain the variability of atmospheric CO_2 and therefore they are crucial to interpret the observations of near surface CO_2 and column-averaged CO_2 (XCO_2) in the MVS. In the CHE project the evaluation of the tier 2 global nature run has shown that large part of the biases in the seasonal cycle of atmospheric CO_2 simulations (Figure 12, upper panels) can be explained by errors in the biogenic fluxes (Figure 12, lower panels and Figure 13, left panels). Overall, the low CO_2 values in the summer are not low enough as shown by the positive bias at the Total Carbon Column Observing Network (TCCON) sites from June to August during which the atmospheric enhancement associated with biogenic fluxes is strongest. This is consistent with the large underestimation of the modelled Net Ecosystem Exchange (NEE) at the ICOS-Ecosystem Thematic Centre (ETC) sites of around 4 μmol $m^{-2}s^{-1}$ on average with respect to eddy covariance observations and the CHE FLUXCOM product (based on Jung et al., 2020). This is attributed to a very large underestimation of Gross Primary Production (GPP) in the model of around 4 μmol $m^{-2}s^{-1}$ on average, but also in ecosystem respiration (Reco) (2 μmol $m^{-2}s^{-1}$) at weekly to monthly timescales. These errors in GPP are consistent with systematic errors in the diurnal cycle during the summer period with an amplitude underestimation of around 5 μmol $m^{-2}s^{-1}$ at the ICOS-ETC sites.

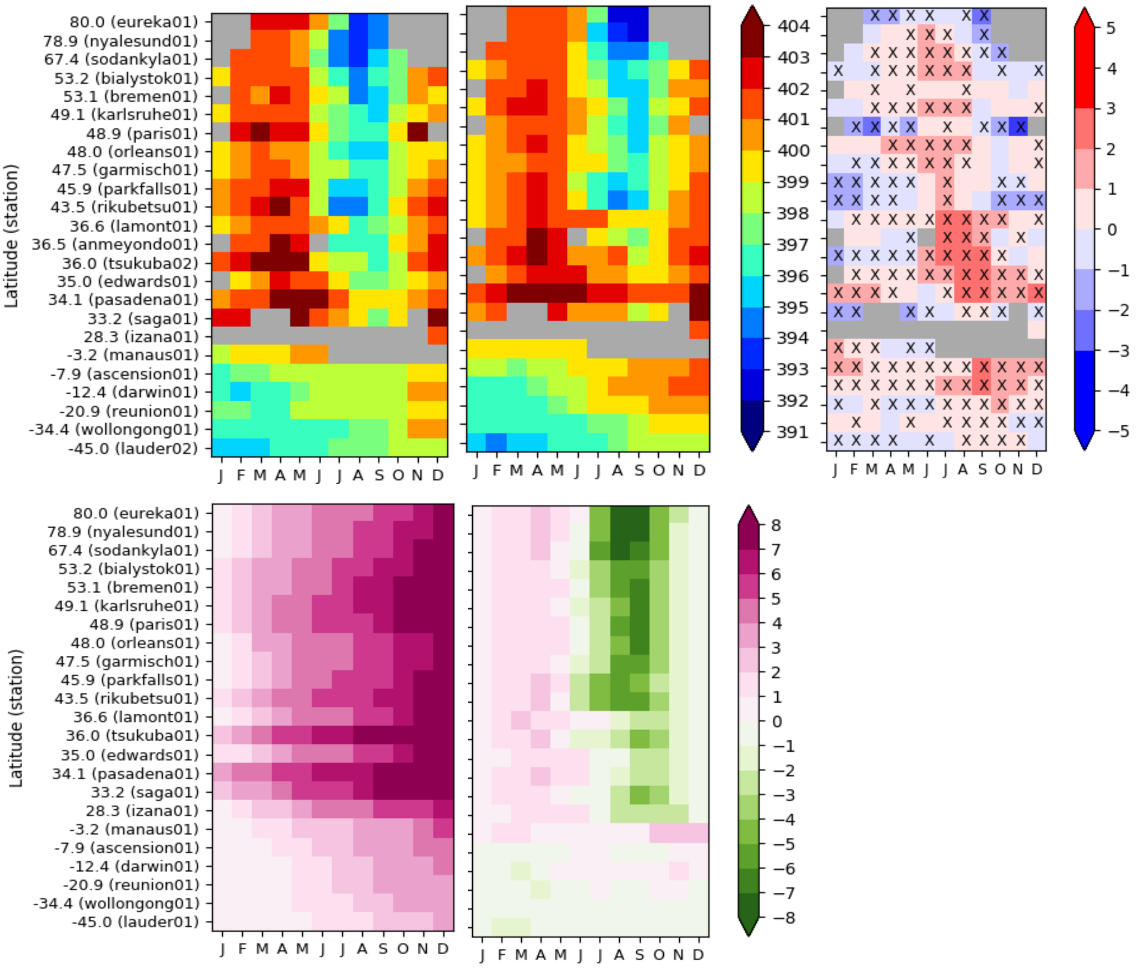

Figure 12 Upper panels: Monthly mean column-averaged CO_2 dry molar fraction (XCO_2) [ppm] from TCCON observation (TCCON Team, 2017) (left) and CHE tier 2 nature run (middle) and the monthly bias of the CHE tier 2 nature run with respect to observations (right). Grey colour indicates no observations are available. Lower panels: Monthly mean XCO_2 accumulated enhancement [ppm] associated with anthropogenic emissions (left) and land biogenic fluxes (right) throughout the CHE tier2 nature run at the same TCCON sites.

The errors in the models used to estimate the prior biogenic fluxes are associated with a wide range of error sources. Important sources of uncertainty are related to the land use and land use change errors as well as the LAI scaling method that allows its disaggregation into high and low vegetation components (Boussetta et al., 2013). This is illustrated in Figure 14 which shows preliminary sensitivity results from experiments performed with the IFS. The experiments compare the use of the new land cover data from ESA-CCI provided by C3S (http://datastore.copernicus-climate.eu/documents/satellite-land-cover/D3.3.12-v1.2_PUGS_ICDR_LC_v2.1.x_PRODUCTS_v1.2.pdf) together with the new LAI scaling method to a control setting based on the operational LAI data (MODIS collection 5 climatology) and the GLCC land cover data (Loveland et al., 2000; http://edcdaac.usgs.gov/glcc/glcc.html). Overall, the results show a large impact of the land cover and LAI on NEE at regional scale. The NEE differences are around 3 μmol $m^{-2}s^{-1}$ in magnitude, with positive and negative differences over various regions. These NEE changes are associated with changes in both GPP and RESP. More work is under way to calibrate model parameters associated with the land surface model using the new land cover and LAI data. However, these preliminary results indicate that these changes would have a significant impact on regional CO_2 budgets which will lead to changes in atmospheric CO_2 gradients.

The ultimate goal of the evaluation of the biogenic flux prior is to understand the source of biogenic flux errors so that we can improve the underlying biogenic model, and to quantify the uncertainty of prior fluxes for future atmospheric inversions based on the IFS. These two aspects will be addressed in the CHE follow on project (CoCO2).

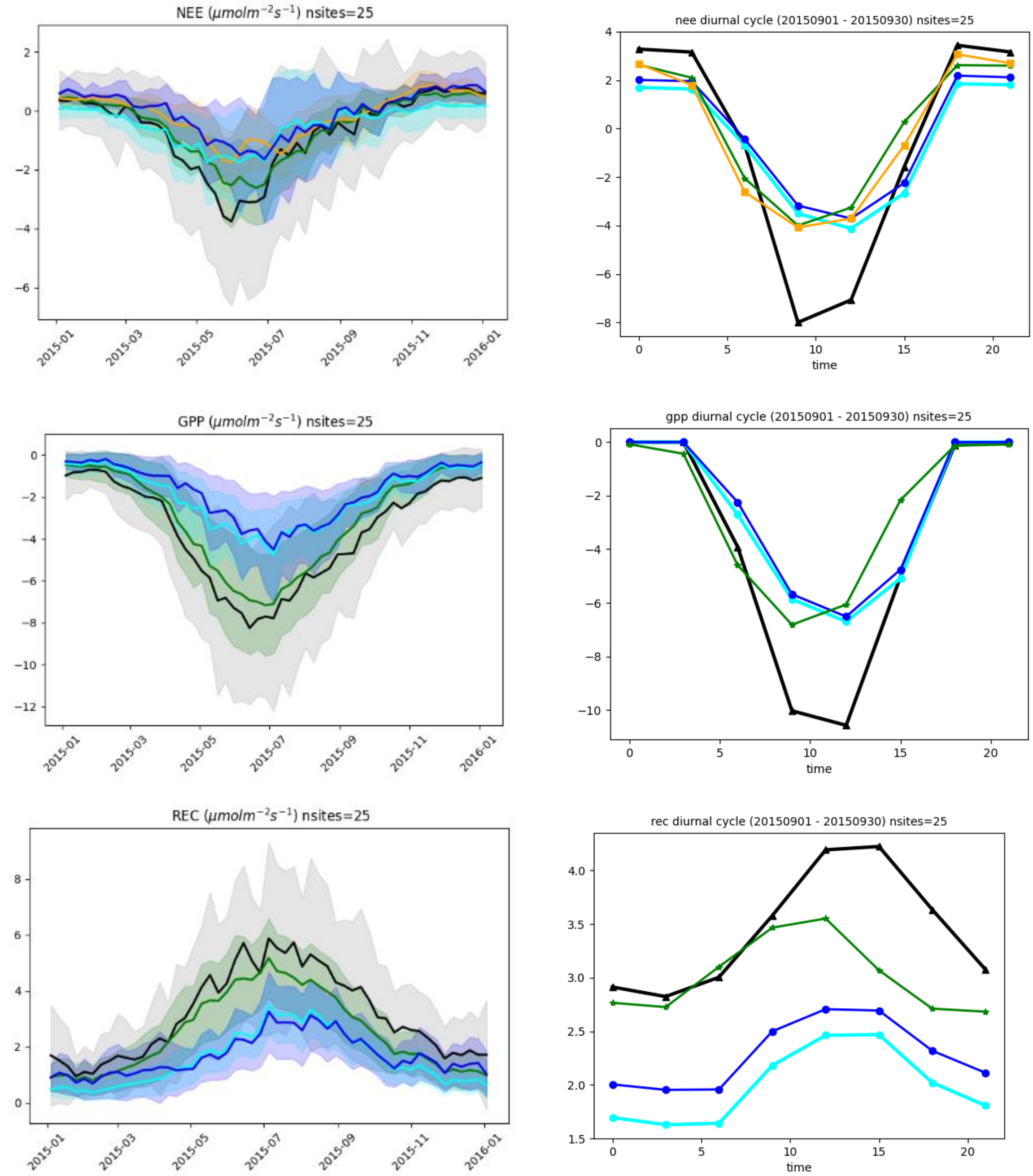

Figure 13 Mean seasonal cycle of NEE (top), GPP (middle) and RESP (bottom) [µmol m2 s-1] at 25 ICOS-ETC Eddy Covariance (EC) sites in 2015 from ICOS Research Infrastructure (2019). Observations are shown in black; the IFS modelled fluxes in cyan and the bias corrected fluxes used in the CHE T2 nature run in blue; the CAMS inversion product (total flux – anthropogenic emissions) based on surface observations is shown in orange; and the CHE FLUXCOM product (based on Jung et al., 2020) in green. the The shading depicts the standard deviation across the 25 sites. Right panels: Median of the diurnal cycle of NEE (left), GPP (middle) and RESP (right) [µmol m2 s-1] at the 25 ICOS-ETC EC sites in July 2015.

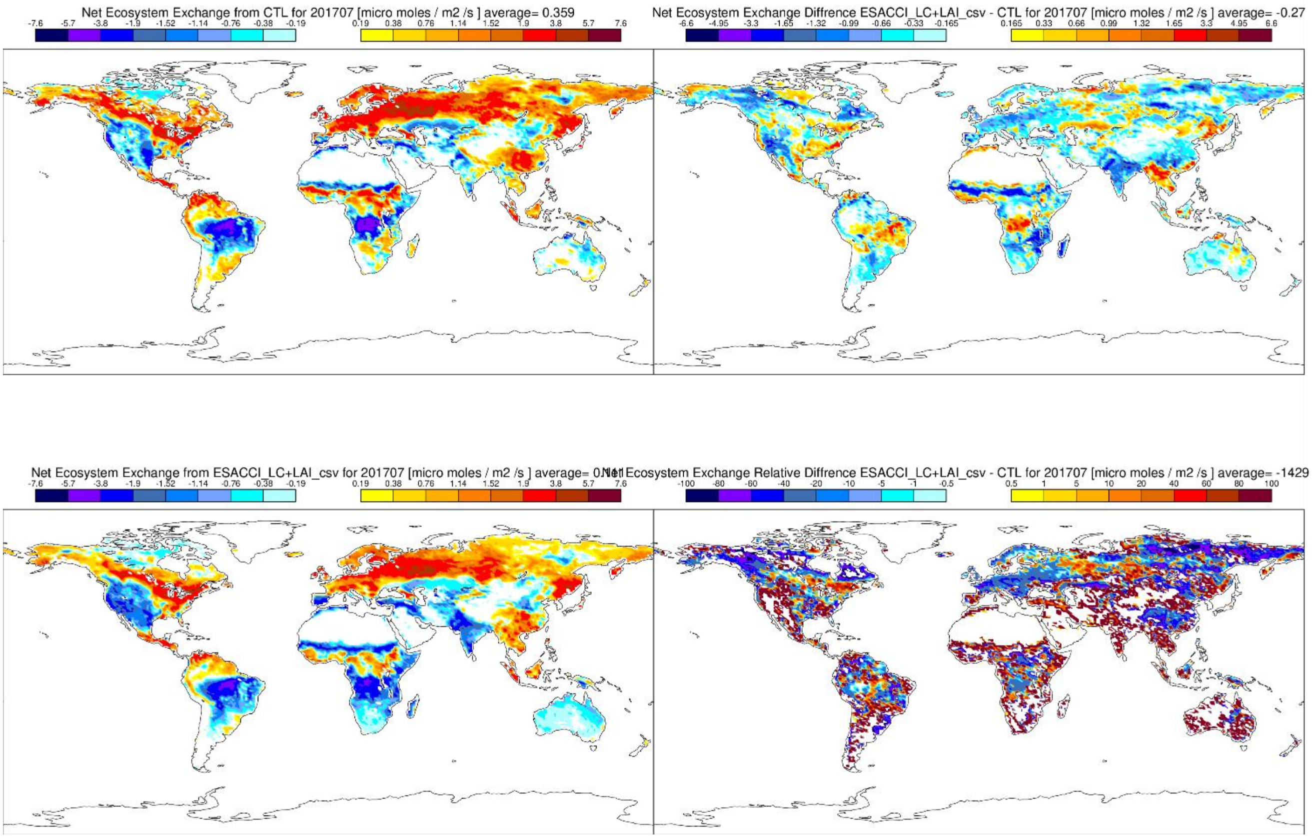

Figure 14 Monthly mean NEE in July 2017 [µmol m-2s-1] from the control experiment using current IFS operational land cover from GLCC and MODIS LAI climatology (top left) and from the ESA-CCI with LAI climatology (lower left). The difference between the two experiments is shown on the top right panel with the relative differences [%] shown in the lower right panel.

5 Recommendations for operational CHE prototype

Three immediate priorities were identified in the CHE WP2-WP5 workshop (organized by EMPA in May 2020) to further develop critical modelling and prior information aspects of the operational CO2MVS prototype:

1. Improve accuracy of tracer transport schemes with emphasis on mass conservation and numerical diffusion/dispersion of tracer advection, and the representation of boundary layer mixing, particularly under stable conditions.
2. Improve spatial and temporal representation of plumes from hotspots with emphasis on vertical and temporal variability of emissions and use of co-emitted species.
3. Improve spatial and temporal representation of biogenic flux priors that largely control the variability of the background CO_2 concentrations.

These topics will be addressed in the CoCO2 project. Detailed recommendations on the different aspects related to these three main priorities are provided in Table 2.

Table 2: Implementation priorities linked to the domain (global, regional,local) and stream for application in the prototype: Near Real Time (NRT), or re-analysis (RA). An estimate of the effort required is given in person months.

Topic identifier	Component	Domain	Stream	Recommendation	Estimated effort (Person Months)
IM-TRA-1	Transport	global regional	NRT RA	Test near mass-conserving advection scheme in online models (e.g. COMAD semi-Lagrangian in the IFS)	6 months
IM-TRA-2	Transport	global regional local	NRT RA	Evaluation of turbulent mixing and convective transport using Radon and other tracers (vertical gradients)	9 months
IM-TRA-3	Transport	global regional	NRT RA	Inter-comparison of global, regional and local models to evaluate local transport by plumes	12 months
IM-AEM-1	Anthropogenic emissions	Local (Point Sources)	RA	Characterisation of emission source with all parameters and have plume model for each or for a group of them (evaluate how to group these into "clumps")	12 to 36 months
IM-AEM-2	Anthropogenic emissions	Global	NRT RA	Introduce online fixed spatio-temporal profiles for different sectors at weekly, daily, hourly scales (e.g. Guevara et al. 2019ab, Nassar et al. 2013).	12 months
IM-AEM-3	Anthropogenic emissions	Global Regional	NRT RA	Vertical profiles of emissions (e.g. Brunner et al. 2019) (emission heights + temperature-dependent injection velocities) implemented and tested in a stepwise	12 months

				fashion with incremental complexity	
IM-AEM-4	Anthropogenic emissions	Global Regional	NRT	Modelled temporal profiles with meteo predictors (e.g. residential heating) to support FFDAS approach.	12 months
IM-BIO-1	Biogenic fluxes	Global Regional Local	RA	Extensive site-level cross-validation model intercomparison excercise where models are run at site-level with site-level measured meteo (and high res satellite data cutouts if needed). This would be really helpful and insightful to judge on the qualities and gaps between GPP and NEE models of different kind and complexity. It would also open doors for estimating the spatial-temporal errors and error covariance parameterisations for the different models.	24 months
IM-BIO-2	Biogenic fluxes	Global Regional	NRT	Test improved high resolution mapping of land use in models: classification, cover, including vegetation mapping (CGLS, Buchhorn et al.,2017; ESA-CCI, 2017; ECOCLIMAP Champeaux et al, 2005; GLCC, Loveland et al., 2000; urban settlement dataset from JRC, Pesaresi et all, 2016)	12 months

IM-BIO-3	Biogenic fluxes	Global Regional	RA	Improve simplified model to use information on SIF	24 months
IM-BIO-4	Biogenic fluxes	Global Regional	RA	Test impact of land use change with simplified, data-driven and DGVM	36 months
IM-BIO-5	Biogenic fluxes	Global Regional	RA	Inter-comparison of DGVM, simplified and data-fusion models (multi-model ensemble to characterise uncertainty)	12 to 24 months
IM-CHM-1	Chemistry	Global Regional	NRT RA	Develop computationally affordable chemistry for co-emitted tracers (NO_2, CO, PM2.5, NMVOC)	36 months

6 Research priorities

Longer-term research priorities with a 5 to 10-year timeline (listed in Table 3) will feed into the development of the operational CO2MVS. These will require further research investment to reach the expected maturity for operational implementation in the CO2MVS.

Table 3: Research priorities linked to the domain (global, regional,local) and stream for application in the prototype: Near Real Time (NRT), or re-analysis (RA). An estimate of the effort required is given in person months.

Topic identifier	Component	Domain	Stream	Recommendation	Estimated effort (Person Months)
RS-TRA-1	Transport	Global Regional	NRT RA	Test new transport schemes developed in NWP, e.g. MPDATA advection in FVM IFS (Kühnline et al, 2019)	36 months
R-TRA-2	Transport	Global Regional Local	NRT RA	Integrate plume rise model in emission hotspots (Guevara et al, 2014, Brunner et al., 2019)	24 months
RS-TRA-3	Transport	Regional Local	NRT RA	Evaluate PBL wind profiles crucial for plume modelling (Sandu et al., 2013)	12 months

RS-AEM-1	Anthropogenic emissions	Global Regional Local	NRT RA	Extend FFDAS approach using all available human activity proxies.	24 months
RS-AEM-2	Anthropogenic emissions	Global	RA	Merge mosaic of regional inventories (Tier 2,3) with global inventory (Tier1, Tier2).	12 months
RS-BIO-1	Biogenic fluxes	Global Regional	NRT RA	Use SIF and COS to constrain biogenic fluxes	24 to 36 months
RS-BIO-2	Biogenic fluxes	Global Regional	RA	Introduce crop modelling and relevant land management information (crop rotation/harvesting, grazing, etc.)	24 to 36 months
RS-TRC-1	Other tracers	Regional		Implementation of APO and radiocarbon in forward/inverse model.	36 months

7 Conclusion

This report presents the options for a high-resolution modelling and prior flux estimation capability in the context of the CHE CO_2 prototype based on: multi-scale (global, regional and local), multi-species (CO_2 and co-emitted species) and multi-stream (NRT and re-analysis) models and products. The outcome of the CHE WP2-WP5 workshop organized by EMPA in May 2020 provided guidance on the refinement of the priorities regarding the operational MVS prototype into three major areas:

- Evaluation of tracer transport with the inter-comparison of global, regional and local models, addressed in CHE (CHE D2.1, CHE D2.2, D2.4, D2.6) with various nature runs. These scales underlay the monitoring of CO2 emissions at global, national and regional scales (Pinty et al, 2017). Undetected biases in the transport will lead to biases in the estimated emissions. Therefore, the continuous evaluation and improvement of the transport accuracy on those scales (from global to plume) is crucial.
- Evaluation of requirements for plume representation in models with case studies of plumes from hotspots using different transport models (e.g. CHE D2.7, D2.8, SMARTCARB). The small scales required to resolve the plume transport and the strong dependency of the plume evolution on the representation of spatial/temporal variability of emissions, the background CO_2 and the meteorological information are challenges that need to be addressed at the model level in the context of the monitoring of emissions from hotspots. These challenges highlight the need for high resolution, human activity data, co-emitted species and fossil fuel emission models in the MVS.

- Inter-comparison of different modelled biogenic products with independent data (e.g. CHE D2.3 and CHE D3.2) from global, regional to local scales in order to quantify uncertainties and to understand the sources of biogenic variability and error. Such activity would help to improve the characterization of the CO_2 background concentration and its variability.

These activities will be further developed in the future CoCO2 project based on specific recommendations collected in this report (section 5) and the accompanying reports of the different building blocks in the CO_2 MVS prototype (CHE D5.2, D5.6, D5.8). All the recommendations will be integrated in a final report (CHE D5.9) for the design of the operational CO_2 MVS prototype.

8 Acronyms

Table 4 List of acronyms

APO	*Atmospheric Potential Oxygen*
CAMS	*Copernicus Atmosphere Monitoring Service*
CASA	*Carnegie-Ames-Stanford Approach*
CFL	*Courant–Friedrichs–Lewy or CFL condition*
CNRM	Centre National de Recherches Météorologiques
COSMO	*Consortium for Small-scale Modeling*
CTM	*Chemical Transport Model*
DGVM	*Dynamic Global Vegetation Model*
ECMWF	*European Centre for Medium Range Weather Forecasts*
EDGAR	*Emissions Database for Global Atmospheric Research*
EEA	*European Environmental Agency*
EMEP	*European Monitoring and Evaluation Programme*
EO	*Earth Observation*
EMPA	*Swiss Federal Laboratories for Materials Science and Technology*
ESA-CCI	*European Space Agency – Climate Change Initiative*
ESM	*Earth System Model*
EULAG	*Eulerian/semi-Lagrangian fluid solver*
FAPAR	*Fraction of Absorbed Photosynthetically Active Radiation*
GEMS	*Global Earth-system Monitoring using Satellite and in-situ data*
GLCC	*Global Land Cover Characterization*
GOBM	*Global Ocean Biogeochemistry Models*
GPP	*Gross Primary Production*
ICOS	*Integrated Carbon Observation System*

IFS	*Integrated Forecasting System*
IEA	*International Energy Agency*
IPCC	*The Intergovernmental Panel on Climate Change*
IPSL	*Institut Pierre Simon Laplace*
LAI	*Leaf Area Index*
LEO	*Low Earth Orbit*
LM	*Lagrangian model*
LMDz	*Laboratoire de Météorologie Dynamique (LMDz) GCM*
LPDM	*Lagrangian Particle Dispersion Models*
LUE	*Light Use Efficiency*
MACC	*Monitoring Atmospheric Composition and Climate*
NASA	*National Aeronautics and Space Administration*
NCAR	*National Center for Atmospheric Research*
NEE	*Net Ecosystem Exchange*
NRT	*Near Real Time*
NWP	Numerical Weather Prediction
ORCHIDEE	*Organising Carbon and Hydrology In Dynamic Ecosystems*
PFT	*Plant Functional Type*
RESP	*Ecosystem Respiration*
SiB	*Simple Biosphere*
SIF	*Solar Induced Fluorescence*
SDBM	*Simple Diagnostic Biosphere Model*
SOCAT	*Surface Ocean CO_2 ATlas*
TCCON	*Total Carbon Column Observing Network*
TNO	*Netherlands Organisation for Applied Scientific Research*
UNFCCC	*United Nations Framework Convention on Climate Change*
VPRM	*Vegetation Photosynthesis and Respiration Model*
WRF	*Weather Research and Forecasting*

9 References

CHE D2.1: Haussaire et al. Model systems and simulation configurations, 2018

CHE D2.2: Agusti-Panareda et al. The CHE tier 1 global nature run, 2018

CHE D2.3: Denier van der Gon et al. Emissions and natural fluxes datasets, 2019

CHE D2.4: Haussaire et al. Regional nature runs, 2019

CHE D2.6: Agusti-Panareda and McNorton, The CHE tier2 global nature run, 2019

CHE D2.8: Klonecki, A., P. Prunet, LES Simulation Report, 2020

CHE D3.2: Walther, S., M. Jung, Net biogenic CO_2 fluxes, 2019

CHE D3.3: Choulga M., and Janssens-Maenhout, G., Global anthropogenic CO2 emission budgets and uncertainties, 2019

CHE D3.4: de Laat and van der A., Fingerprints of fossil CO_2 sources, 2019

CHE D4.1: Marshall, J., Current European in-situ atmospheric measurement capacity, 2018

CHE D4.3: Marshall, J., Nunez Ramirez, T.,Attribution problem configurations, 2019

CHE D5.2: Chevallier, F., Final report on service elements for CO_2 Earth observation integration, 2020

CHE D5.6: Peters, W., M. Krol, Final report on service elements for data assimilation methodology, 2020

CHE D5.8: Scholze, M. H. Chen, Final report on service element requirements for uncertainty representation, 2020

CHE D5.9: Balsamo, G., CHE WP leaders: Final report on service elements for an integrated CHE monitoring infrastructure, 2020.

Agustí-Panareda, A. et al. (2014): Forecasting global atmospheric CO_2, Atmos. Chem. Phys., 14, 11959–11983, https://doi.org/10.5194/acp-14-11959-2014

Agustí-Panareda, A. et al. (2016): A biogenic CO_2 flux adjustment scheme for the mitigation of large-scale biases in global atmospheric CO_2 analyses and forecasts, Atmos. Chem. Phys., 16, 10399–10418, https://doi.org/10.5194/acp-16-10399-2016

Agustí-Panareda. A. et al. (2019): Modelling CO_2 weather – why horizontal resolution matters, Atmos. Chem. Phys., 19, 7347–7376, https://doi.org/10.5194/acp-19-7347-2019

Aumont, O. and Bopp, L. (2006): Globalizing results from ocean in situ iron fertilization studies, Global Biogeochem. Cy., 20, GB2017, https://doi.org/10.1029/2005GB002591

Basu, S. et al. (2018): The impact of transport model differences on CO_2 surface flux estimates from OCO-2 retrievals of column average CO_2, Atmos. Chem. Phys., 18, 7189–7215, https://doi.org/10.5194/acp-18-7189-2018

Belikov, D. A. et al. (2013): Off-line algorithm for calculation of vertical tracer transport in the troposphere due to deep convection, Atmos. Chem. Phys., 13, 1093-1114, https://doi.org/10.5194/acp-13-1093-2013

Best, M.J., (2005): Representing urban areas within operational numerical weather prediction models. Boundary-Layer Meteorology, 114(1), pp.91-109

Berthet, S. et al. (2019).: Evaluation of an Online Grid-Coarsening Algorithm in a Global Eddy-Admitting Ocean Biogeochemical Model, ournal of Advances in Modeling Earth Systems, 11, 1759– 1783. https://doi.org/10.1029/2019MS001644

Bieser, J. et al. (2011): Vertical emission profiles for Europe based on plume rise calculations, Environ. Pollut., 159, 2935–2946,https://doi.org/10.1016/j.envpol.2011.04.030

Bodesheim, P. et al. (2018): Upscaled diurnal cycles of land–atmosphere fluxes: a new global half-hourly data product, Earth System Science Data, 10 (3), 1327-1365

Boussetta, S. et al. (2013): Natural land carbon dioxide exchanges in the ECMWF integrated forecasting system: Implementation and offline validation, *J. Geophys. Res. Atmos.*, 118, 5923– 5946, doi:10.1002/jgrd.50488

Brunner, D. et al. (2019): Accounting for the vertical distribution of emissions in atmospheric CO_2 simulations, Atmos. Chem. Phys., 19, 4541–4559, https://doi.org/10.5194/acp-19-4541-2019

Buchhorn, M. et al. (2017): Copernicus Global Land Operations "Vegetation and Energy": Algorithm Theoretical Basis Document for Moderate Dynamic Land Cover, https://land.copernicus.eu/global/sites/cgls.vito.be/files/products/CGLOPS1_ATBD_LC100m-V1_I1.00.pdf

Buitenhuis, E. T. et al. (2010): Biogeochemical fluxes through microzooplankton, Global Biogeochem. Cy., 24, GB4015, https://doi.org/10.1029/2009GB003601

Cai, B. et al. (2018) : China high resolution emission database (CHRED) with point emission sources, gridded emission data, and supplementary socioeconomic data, Resources, Conservation and Recycling, Vol. 129, Pages 232-239

Chambers, S. D., Williams, A. G., Crawford, J., and Griffiths, A. D.: On the use of radon for quantifying the effects of atmospheric stability on urban emissions, Atmos. Chem. Phys., 15, 1175–1190, https://doi.org/10.5194/acp-15-1175-2015, 2015

Champeaux J.L. et al. (2005) : ECOCLIMAP : a global database of land surface parameters at 1km resolution, Met. Apps, 12: 29-32. doi:10.1017/S1350482705001519

Chevallier, F., et al. (2012), What eddy-covariance measurements tell us about prior land flux errors in CO_2 -flux inversion schemes, Global Biogeochem. Cycles, 26, GB1021, doi:10.1029/2010GB003974

Choulga, M., et al. (2020): Global anthropogenic CO2 emissions and uncertainties as prior for Earth system modelling and data assimilation, Earth Syst. Sci. Data Discuss., https://doi.org/10.5194/essd-2020-68, in review

Denning, A.S., et al. (1999) Can a strongatmospheric CO2 rectifier effect be reconciled with a "reasonable" carbon budget?, Tellus B:Chemical and Physical Meteorology, 51:2, 249-253, DOI: 10.3402/tellusb.v51i2.16277

Denier van der Gon, H. et al. (2011): Description of current temporal emission patterns and sensitivity of predicted AQ for temporal emission patterns, TNO report, EU FP7 MACC deliverable report D_D-EMIS_1.3; https://atmosphere.copernicus.eu/sites/default/files/2019-07/MACC_TNO_del_1_3_v2.pdf

Diamantakis, M. (2014): The semi-Lagrangian technique in atmospheric modelling:current status and future challenges, ECMWF Annual Seminar Proceedings, https://www.ecmwf.int/sites/default/files/elibrary/2014/9054-semi-lagrangian-technique-atmospheric-modelling-current-status-and-future-challenges.pdf

Doney, S. C. et al. (2009): Mechanisms governing interannual variability in upper-ocean inorganic carbon system and air–sea CO_2 fluxes: Physical climate and atmospheric dust, Deep-Sea Res. Pt. II, 56, 640–655, https://doi.org/10.1016/j.dsr2.2008.12.006

Eskes, H. et al. (2019): Sentinel-5 precursor/TROPOMI Level 2 Product User Manual Nitrogendioxide, Tech. Rep. S5P-KNMI-L2-0021-MA, Koninklijk Nederlands Meteorologisch Instituut (KNMI), https://sentinels.copernicus.eu/documents/247904/2474726/Sentinel-5P-Level-2-Product-User-Manual-Nitrogen-Dioxide, CI-7570-PUM, issue 3.0.0

Farquhar, G.D. et al. (1980): A biochemical model of photosynthetic CO_2 assimilation in leaves of C3 species, Planta149:78–90

Fiehn, A. et al. (2020): Estimating CH4, CO2, and CO emissions from coal mining and industrial activities in the Upper Silesian Coal Basin using an aircraft-based mass balance approach, Atmos. Chem. Phys. Discuss., https://doi.org/10.5194/acp-2020-282, in review

Feng, L. et al. (2011): Evaluating a 3-D transport model of atmospheric CO_2 using ground-based, aircraft, and space-borne data, Atmos. Chem. Phys., 11, 2789–2803, doi:10.5194/acp-11-2789-2011

Flemming, J. et al. (2015): Tropospheric chemistry in the Integrated Forecasting System of ECMWF, Geosci. Model Dev., 8, 975–1003, https://doi.org/10.5194/gmd-8-975-2015

Freitas, S. R. et al. (2007): Including the sub-grid scale plume rise of vegetation fires in low resolution atmospheric transport models, Atmos. Chem. Phys., 7, 3385-3398, https://doi.org/10.5194/acp-7-3385-2007

Friedlingstein, P. et al. (2006): Climate–carbon cycle feedback analysis: Results from the C4MIP model intercomparison. J. Climate, 19, 3337–3353

Friedlingstein P. et al. (2019): Global Carbon Budget 2019, Earth Syst. Sci. Data, 11, 1783–1838, https://doi.org/10.5194/essd-11-1783-2019

Gaubert, B. et al. (2019): Global atmospheric CO_2 inverse models converging on neutral tropical land exchange, but disagreeing on fossil fuel and atmospheric growth rate, Biogeosciences, 16, 117–134, https://doi.org/10.5194/bg-16-117-2019

Gaudet, BJ, et al. (2017): Exploration of the impact of nearby sources on urban atmospheric inversions using large eddy simulation. Elem Sci Anth, 5: 60. DOI:https://doi.org/10.1525/elementa.247

Gavete, L. et al. (2012): Implementation in CHIMERE of a conservative solver for the advection equation – cmmse10, Journal of Computational and Applied Mathematics, Vol. 236, 12, 3026-3033.S

Goret, M. et al. (2019): Inclusion of CO_2 flux modelling in an urban canopy layer model and an evaluation over an old European city centre. Atmospheric Environment: X, 3, p.100042

Guevara, M. et al. (2013): An improved system for modelling Spanish emissions: HERMESv2. 0. Atmospheric environment, 81, pp.209-221

Guevara, M. et al. (2014): Implementation of plume rise and its impacts on emissions and air quality modelling, Atmos. Environ., 99, 618–629,https://doi.org/10.1016/j.atmosenv.2014.10.029

Guevara, M. et al. (2019a): HERMESv3, a stand-alone multi-scale atmospheric emission modelling framework – Part 1: global and regional module, Geosci. Model Dev., 12, 1885–1907, https://doi.org/10.5194/gmd-12-1885-2019, 2019

Guevara, M. et al. (2019b): HERMESv3, a stand-alone multi-scale atmospheric emission modelling framework – Part 2: The bottom–up module, Geosci. Model Dev., 13, 873–903, https://doi.org/10.5194/gmd-13-873-2020, 2020

Gurney, K. R. et al. (2003): TransCom 3 CO_2 inversion intercomparison: 1. Annual mean control results and sensitivity to transport and prior flux information. Tellus B, 55: 555-579. doi:10.1034/j.1600-0889.2003.00049.x

Gurney, K.R. et al. (2009): The Vulcan Project: High resolution fossil fuel combustion CO_2 emissions fluxes for the United States, Environ. Sci. Technol., 43, doi:10.1021/es900,806c

Gurney, K. R. et al. (2019): The Hestia fossil fuel CO2 emissions data product for the Los Angeles megacity (Hestia-LA), Earth Syst. Sci. Data, 11, 1309–1335, https://doi.org/10.5194/essd-11-1309-2019

Hauck, J. et al. (2016): ron fertilisation and century-scale effects of open ocean dissolution of olivine in a simulated CO_2 removal experiment, Environ. Res. Lett., 11, 024007, https://doi.org/10.1088/1748-9326/11/2/024007

Huijnen, V. et al. (2019): Quantifying uncertainties due to chemistry modelling – evaluation of tropospheric composition simulations in the CAMS model (cycle 43R1), Geosci. Model Dev., 12, 1725–1752, https://doi.org/10.5194/gmd-12-1725-2019

ICOS Research Infrastructure (2019). Ecosystem eddy covariance final quality (L2) flux product in ETC-Archive format -release 2019-1 (Version 1.0). ICOS Carbon Portal. https://doi.org/10.18160/NNAD-PN5W, 4 July 2019

Inness, A. et al.(2019): The CAMS reanalysis of atmospheric composition, Atmos. Chem. Phys., 19, 3515–3556, https://doi.org/10.5194/acp-19-3515-2019

Jacobs, C. M. et al. (1996), Stomatal behaviour and photosynthetic rate of unstressed grapevines in semi-arid conditions, Agric. For. Meteorol., 80, 111–134

Jacobs, C. M. J., et al. (2007), Variability of annual CO_2 exchange from Dutch grasslands, Biogeosci., 4, 803–816

Janssens-Maenhout, G. et al. (2019): EDGAR v4.3.2 Global Atlas of the three major greenhouse gas emissions for the period 1970–2012, Earth Syst. Sci. Data, 11, 959–1002, https://doi.org/10.5194/essd-11-959-2019

Janssens-Maenhout, G. et al. (2015): HTAP_v2.2: a mosaic of regional and global emission grid maps for 2008 and 2010 to study hemispheric transport of air pollution, Atmos. Chem. Phys., 15, 11411-11432, doi:10.5194/acp-15-11411-2015

Joiner, J. et al., (2018): Estimation of Terrestrial Global Gross Primary Production (GPP) with Satellite Data-Driven Models and Eddy Covariance Flux Data. *Remote Sens.*, *10*, 1346

Jung, M., et al. (2017): Compensatory water effects link yearly global land CO_2 sink changes to temperature, Nature, 541(7638), 516-520

Jung, M., Schwalm, C., Migliavacca, M., Walther, S., Camps-Valls, G., Koirala, S., Anthoni, P., Besnard, S., Bodesheim, P., Carvalhais, N., Chevallier, F., Gans, F., Goll, D. S., Haverd, V., Köhler, P., Ichii, K., Jain, A. K., Liu, J., Lombardozzi, D., Nabel, J. E. M. S., Nelson, J. A., O'Sullivan, M., Pallandt, M., Papale, D., Peters, W., Pongratz, J., Rödenbeck, C., Sitch, S., Tramontana, G., Walker, A., Weber, U., and Reichstein, M.: Scaling carbon fluxes from eddy covariance sites to globe: synthesis and evaluation of the FLUXCOM approach, Biogeosciences, 17, 1343–1365, https://doi.org/10.5194/bg-17-1343-2020, 2020

Kaminski, T. et al. (2017): Constraining a terrestrial biosphere model with remotely sensed atmospheric carbon dioxide. Remote Sensing of Environment, doi:10.1016/j.rse.2017.08.017

Karion, A., et al. (2019).: Intercomparison of atmospheric trace gas dispersion models: Barnett Shale case study, Atmos. Chem. Phys., 19, 2561–2576, https://doi.org/10.5194/acp-19-2561-2019

Keller, C. A. et al. (2014): HEMCO v1.0: a versatile, ESMF-compliant component for calculating emissions in atmospheric models, Geosci. Model Dev., 7, 1409–1417, https://doi.org/10.5194/gmd-7-1409-2014

Knorr, W. and M. Heimann (1995): Impact of drought stress and other factors on seasonal land biosphere CO_2 exchange studied through an atmospheric tracer transport model. Tellus B, 47: 471-489. doi:10.1034/j.1600-0889.47.issue4.7.x

Kuhlmann, G., et al. (2019): Detectability of CO2 emission plumes of cities and power plants with the Copernicus Anthropogenic CO2 Monitoring (CO2M) mission, Atmos. Meas. Tech., 12, 6695–6719, https://doi.org/10.5194/amt-12-6695-2019

Kuhlmann, G., et al. (2020) Quantifying CO2 emissions of a city with the Copernicus Anthropogenic CO2 Monitoring satellite mission, Atmos. Meas. Tech. Discuss., https://doi.org/10.5194/amt-2020-162, in review

Kühnlein, C. et al. (2019).: FVM 1.0: a nonhydrostatic finite-volume dynamical core for the IFS, Geosci. Model Dev., 12, 651–676, https://doi.org/10.5194/gmd-12-651-2019

Landschützer, P. et al. (2015). The reinvigoration of the Southern Ocean carbon sink, Science, 349, 1221-1224. doi: 10.1126/science.aab2620

Launois, T. et al. (2015).: A new model for the global biogeochemical cycle of carbonyl sulfide – Part 1: Assessment of direct marine emissions with an oceanic general circulation and biogeochemistry model, Atmos. Chem. Phys., 15, 2295–2312, https://doi.org/10.5194/acp-15-2295-2015

Law, R. M., et al. (2008): TransCom model simulations of hourly atmospheric CO_2: Experimental overview and diurnal cycle results for 2002, Global Biogeochem. Cycles, 22, GB3009, doi:10.1029/2007GB003050

Law. R. M. et al. (1996): Variations in modelled atmospheric transport of carbon dioxide and the consequences for CO_2 inversions. Global Biogeochemical Cycles, 10, 783-796

Le Quéré, C. et al. (2018): Global Carbon Budget 2018, Earth Syst. Sci. Data, 10, 2141–2194, https://doi.org/10.5194/essd-10-2141-2018

Lin, J. C. et al. (2011): Studying atmospheric transport through Lagrangian models, Eos Transactions, 92(21), 177-184

Lin, J. C. et al. (2003), A near-field tool for simulating the upstream influence of atmospheric observations: The Stochastic Time-Inverted Lagrangian Transport (STILT) model, J. Geophys. Res., 108, 4493, doi:10.1029/2002JD003161, D16

Liu, Y. et al. (2017): Spatiotemporal patterns of the fossil-fuel CO_2 signal in central Europe: results from a high-resolution atmospheric transport model, Atmos. Chem. Phys., 17, 14145–14169, https://doi.org/10.5194/acp-17-14145-2017

Loveland, T.R. et al. (2000): Development of a global land cover characteristics database and IGBP DISCover from 1 km AVHRR data, International Journal of Remote Sensing, 21:6-7, 1303-1330, DOI: 10.1080/014311600210191

Mahadevan, P. et al. (2008): A satellite-based biosphere parameterization for net ecosystem CO2 exchange: Vegetation Photosynthesis and Respiration Model (VPRM), Global biochemical cycles, 22, 2, doi: 10.1029/2006GB002735

Malardel, S. and Ricard, D. (2015), An alternative cell-averaged departure point reconstruction for pointwise semi-Lagrangian transport schemes. Q.J.R. Meteorol. Soc, 141: 2114-2126. doi:10.1002/qj.2509

Masson, V. (2000): A physically-based scheme for the urban energy budget in atmospheric models. Boundary-layer meteorology, 94(3), pp.357-397

Matthias, V. et al. (2018): Modeling emissions for three-dimensional atmospheric chemistry transport models. Journal of the Air & Waste Management Association, 1-38

Mauritsen, T. et al. (2019): A Developments in the MPI-M Earth System Model version 1.2 (MPI-ESM1.2) and its response to increasing CO2, Journal of Advances in Modeling Earth Systems, 11, 998– 1038. https://doi.org/10.1029/2018MS001400

McGrath-Spangler, E. L. et al. (2015): Impact of planetary boundary layer turbulence on model climate and tracer transport, Atmos. Chem. Phys., 15, 7269–7286, https://doi.org/10.5194/acp-15-7269-2015

McNorton, J. R., et al. (2020): Representing model uncertainty for global atmospheric CO2 flux inversions using ECMWF-IFS-46R1, Geosci. Model Dev., 13, 2297–2313, https://doi.org/10.5194/gmd-13-2297-2020

McNorton, J.R. et al. (2020): Implementation of an urban scheme within the IFS, Journal for Advances in Earth Systems, in preparation

Nassar, R.L. et al. (2013): Improving the temporal and spatial distribution of CO 2 emissions from global fossil fuel emission data sets, J. Geophys. Res. Atmos.,118, 917–933, doi:10.1029/2012JD018196

Patra, P. K., et al. (2008), TransCom model simulations of hourly atmospheric CO2: Analysis of synoptic-scale variations for the period 2002–2003, Global Biogeochem. Cycles, 22, GB4013, doi:10.1029/2007GB003081

Pesaresi, M. et al. (2016): Assessment of the added-value of Sentinel-2 for detecting built-up areas, Remote Sens. 2016, 8(4), 299; https://doi.org/10.3390/rs8040299

Pinty B. et al. (2017): An Operational Anthropogenic CO2 Emissions Monitoring & Verification Support capacity -Baseline Requirements, Model Components and Functional Architecture, doi: 10.2760/08644, European Commission Joint Research Centre, EUR 28736 EN

Pisso, I. et al. (2019): The Lagrangian particle dispersion model FLEXPART version 10.4, Geosci. Model Dev., 12, 4955–4997, https://doi.org/10.5194/gmd-12-4955-2019

Porson, A. et al. (2010): Implementation of a new urban energy budget scheme into MetUM. Part II: Validation against observations and model intercomparison. Quarterly Journal of the Royal Meteorological Society, 136(651), pp.1530-1542

Pouliot, G. et al. (2012): Comparing Emissions Inventories and Model-Ready Emissions Datasets between Europe and North America for the AQMEII Project. Atmospheric Environment (AQMEII issue) 53, 4–14

Rayner, P. J. and Law, R. M. (1995): A comparison of modelled responses to prescribed CO_2 sources. CSIRO Division of Atmospheric Research Technical Paper No. 36

Rayner, P. J. et al. (2010), A new global gridded data set of CO_2 emissions from fossil fuel combustion: Methodology and evaluation, J. Geophys. Res., 115, D19306, doi:10.1029/2009JD013439

Remaud, M. et al. (2018): On the impact of recent developments of the LMDz atmospheric general circulation model on the simulation of CO2 transport, Geosci. Model Dev., 11, 4489–4513, https://doi.org/10.5194/gmd-11-4489-2018

Rödenbeck, C., et al. (2013).: Global surface-ocean pCO2 and sea–air CO2 flux variability from an observation-driven ocean mixed-layer scheme, Ocean Sci., 9, 193–216, https://doi.org/10.5194/os-9-193-2013

Rödenbeck, C. et al. (2014): Interannual sea–air CO2 flux variability from an observation-driven ocean mixed-layer scheme, Biogeosciences, 11, 4599–4613, https://doi.org/10.5194/bg-11-4599-2014

Running, S.W. et al. (2004): A continuous satellite-derived measure of global terrestrial primary production, BioScience, Vol. 54 (6)

Sandu, I. et al. (2013): Why is it so difficult to represent stably stratified conditions in numerical weather prediction (NWP) models?, J. Adv. Model. Earth Syst., 5, 117– 133, doi:10.1002/jame.2013

Schmidt, M. et al. (2014): High-precision quasi-continuous atmospheric greenhouse gas measurements at Trainou tower (Orléans forest, France), Atmos. Meas. Tech., 7, 2283–2296, https://doi.org/10.5194/amt-7-2283-2014

Schneider, W. and Bott, A. (2014). On the time-splitting errors of one-dimensional advection schemes in numerical weather prediction models; a comparative study. Q.J.R. Meteorol. Soc., 140: 2321-2329. doi:10.1002/qj.2301

Sitch, S., et al. (2008): Evaluation of the terrestrial carbon cycle, future plant geography and climate-carbon cycle feedbacks using 5 Dynamic Global Vegetation Models (DGVMs). Global Change Biology, doi: 10.1111/j.1365-2486.2008.01626.x

Sitch, S. et al. (2015): Recent trends and drivers of regional sources and sinks of carbon dioxide, Biogeosciences, 12, 653–679, https://doi.org/10.5194/bg-12-653-2015

Stephens B.B., et al. (2007) Weak northern and strong tropical land carbon uptakefrom vertical profiles of atmospheric CO2.Science316(5832):1732–1735

Schwinger, J. et al. (2016): Evaluation of NorESM-OC (versions 1 and 1.2), the ocean carbon-cycle stand-alone configuration of the Norwegian Earth System Model (NorESM1), Geosci. Model Dev., 9, 2589–2622, https://doi.org/10.5194/gmd-9-2589-2016.

Total Carbon Column Observing Network (TCCON) Team. (2017). 2014 TCCON Data Release (Version GGG2014) [Data set]. CaltechDATA. https://doi.org/10.14291/TCCON.GGG2014

Tramontana, G. et al. (2016): Predicting carbon dioxide and energy fluxes across global FLUXNET sites with regression algorithms. Biogeosciences 13, 4291-4313

Wang, Y. (2016): The potential of observations of radiocarbon in atmospheric CO2 for the atmospheric inversion of fossil fuel CO2 emission at regional scale. Université Paris-Saclay, Paris

Wang, Y. et al. (2018): Potential of European 14 CO 2 observation network to estimate the fossil fuel CO 2 emissions via atmospheric inversions. Atmospheric Chemistry and Physics, 18(6), 4229–4250. http://doi.org/10.5194/acp-18-4229-2018-supplement

Wang, H. (2009): Evaluation of Scalar Advection Schemes in the Advanced Research WRF Model Using Large-Eddy Simulations of Aerosol–Cloud Interactions, Mon. Weather Rev., 137(8), 2547-2558, https://doi.org/10.1175/2009MWR2820.1

Williams, A. G., et al. (2011): The Vertical Distribution of Radon in Clear and Cloudy Daytime Terrestrial Boundary Layers. J. Atmos. Sci., 68, 155–174, https://doi.org/10.1175/2010JAS3576.1

Yu, K. et al. (2018): Errors and improvements in the use of archived meteorological data for chemical transport modeling: an analysis using GEOS-Chem v11-01 driven by GEOS-5 meteorology, Geosci. Model Dev., 11, 305–319, https://doi.org/10.5194/gmd-11-305-2018

Zerroukat, M. (2010). A simple mass conserving semi-Lagrangian scheme for transport problems, J. Comp. Phys., 229(24), 9011-9019, https://doi.org/10.1016/j.jcp.2010.08.017

Document History

Version	Author(s)	Date	Changes
V1.0	Anna Agusti-Panareda et al.	25/11/2019	First draft shared with CHE consortium
V2.0	Anna Agusti-Panareda, Dominik Brunner et al.	6/12/2019	Input of WP leaders and CHE consortium
V3.0	Anna Agusti-Panareda, Dominik Brunner et al.	9/12/2019	Internal review
V4.0	Anna Agusti-Panareda, Dominik Brunner et al.	19/12/2019	Revised report with feedback from reviewers (R. Munro and A. Webb)

Internal Review History

Internal Reviewers	Date	Comments
R. Munro (EUMETSAT)	13/12/2019	Positive review of preliminary report with recommendations to check acronyms and introduce identifiers for the individual recommendations
A.Webb (U. Leicester)	17/12/2019	Positive review of preliminary report with no specific requests.
M. Buchwitz (U. Bremen)	23/09/2019	Constructive review of final report with suggestions to emphasize the integration aspect of the different components
A.Klonecki (SPACIA)	28/09/2019	Positive review of final report with feedback on recommendations

Estimated Effort Contribution per Partner

Partner	Effort
ECMWF	4
EMPA	1.0
JRC	0.5
TNO	0.25
MPI-BGC	0.25
LSCE	0.25
iLab	0.25
WU	0.25
SPASCIA	0.25
Total	**7**